Symmetry vs. asymmetry of a hyper-thinned rift: Example of the Mauleon Basin (Western Pyrenees, France)

Nicolas Saspiturry, Philippe Razin, Thierry Baudin, Olivier Serrano, Benoit Issautier, Eric Lasseur, Cécile Allanic, Isabelle Thinon, Sophie Leleu

Title: Symmetry Vs. Asymmetry of a hyper-thinned rift: example of the *Mauléon* Basin (*Western Pyrenees*, *France*)

Nicolas Saspiturry[1*], Philippe Razin[1], Thierry Baudin[2], Olivier Serrano[2], Benoit Issautier[2], Eric Lasseur[2], Cécile Allanic[2], Isabelle Thinon[2], Sophie Leleu[1]

[1] *Université Bordeaux Montaigne / EA 4592 Géoressources & Environnement, 1 allée Fernand Daguin, 33607 Pessac cedex, France*

[2] *BRGM-French Geological Survey, 3 Avenue Claude Guillemin, 45100 Orléans, France*

**Corresponding author (e-mail: saspiturry.nicolas@gmail.com)*

Abstract

The aim of this study is to unravel the tectono-sedimentary evolution of a hyper-thinned rift, based on the example of the *Mauléon* Basin, a basin filled by thick synrift deposits. The integrated study combines field data, detailed geological mapping and seismic interpretation. The field study focuses on the Iberian margin of the *Mauléon* Basin. Seismic interpretation and well calibration along a N-S transect of the *Mauléon* Basin enable imaging the transition with the northern conjugate margin. The synrift records are very different on either side of the basin: the southern margin is composed of a proximal turbiditic s.l. siliciclastic system, whereas the northern margin is characterized by a carbonate system extending from the platform to the basin. We recognize the *Mauléon* rift as an apparent symmetric hyper-thinned rift, related to a southward dipping Albian detachment and a northward dipping Cenomanian one. Two stages of continental crustal thinning are inferred to explain the development of the *Mauléon* Basin. First, a Barremian to earliest Albian "ductile pure-shear thinning phase", responsible for the lower crustal thinning and the formation of a symmetric sag basin. Second, an Albian-Cenomanian simple-shear thinning phase, responsible for the onset of the southward dipping *Saint-Palais* detachment faulting and for evolution to an asymmetric basin. The Iberian margin appears as an upper plate and the European one as a lower plate during Albian time. At Early Cenomanian time, the basin was affected by structural changes of the

margins resulting from shift in detachment direction, interpreted as "flip-flop detachment tectonics".

Key words: Hyper-extended rift - Pyrenees - Detachment faulting - Mauléon Basin - Early Cretaceous.

1. Introduction

Since the 1980's, conceptual rifting models have evolved from the pure-shear model (McKenzie, 1978), to the simple-shear model (Wernicke 1981, 1985; Wernicke & Burchfiel 1982; Davis, 1983; Spencer 1984; Davis *et al*. 1986; Wernicke & Axen 1988; Brun & van den Driessche 1994) and, more recently, to numerical polyphasing models (Huismans and Beaumont, 2003, 2008, 2011, 2014; Tirel et al., 2004; Lavier and Manatschal, 2006; Brune et al., 2014, 2016; Svartman Dias et al., 2015). Much recent work describes the crustal thinning and modalities of mantle exhumation at actual hyper-thinned passive margins such as the Iberia-Newfoundland (Péron-Pinvidic et al., 2007; Haupert et al., 2016), Angola-Brazil (Unternehr et al., 2010; Péron-Pinvidic et al., 2015), and Australia-Antarctic (Gillard et al., 2015) margins. These have been modelled numerically in order to reproduce the geometry of the continental margins and to understand the development of crustal thinning detachment faults. Although the distal part of these extensional systems is well constrained offshore by seismic interpretation, few studies currently describe the proximal onshore domain. One of the most studied examples is the Jurassic Adriatic margin in the Alps (Masini et al., 2011, 2012, 2013). These authors describe the crustal detachment faults and sedimentary evolution of this starved system. Unlike the situation in the *Mauléon* rift basin, the hyper-thinning crustal models are based on real continental margins bordering oceanic domains. Where the *Pyrenees* are concerned, development of these conceptual models has led some authors to propose different models to explain the location of the Pyrenean mantle outcrops (Lagabrielle

& Bodinier 2008, Jammes *et al*. 2009, 2010a, 2010b; Lagabrielle *et al*. 2010, 2016; Clerc & Lagabrielle, 2014; Masini *et al*. 2014; Tugend *et al*. 2015a; Corre *et al*. 2016; Hart *et al*. 2016; Teixell *et al*. 2016). However, most of the hyper-thinning crustal models are based on mature passive continental margins characterized by mantle exhumation at the ocean-continent transition. The *Mauléon* Basin is an exceptional "laboratory" for the unravelling of the tectono-sedimentary evolution of a highly subsiding, thick, sedimentary, hyper-thinned rift. The evolution of this basin is synchronous to that of the hyper-thinned *Parentis* rift basin (Pinet *et al*. 1987; Bois & ECORS Scientific team 1990; Jammes *et al*. 2010b, Ferrer *et al*. 2012; Masini *et al*. 2014) and to that of the *Bay of Biscay* continental margins, which are characterized by a hyper-thinned continental crust and a probably exhumed mantle at the ocean-continent transition (Ferrer et al., 2008; Roca et al., 2011; Tugend et al., 2014). Even though the *Mauléon* Basin was inverted during the Pyrenean orogeny, it has retained the tectono-sedimentary record from its creation to its reactivation. Recently published geodynamical models of the *Mauléon* Basin are mainly based on structural observations. The aim of this article is to analyze the stratigraphic and sedimentological characteristics of the syn-thinning deposits recording hyper-extension. This approach will make it possible to test the validity of the various models proposed and to bring new elements of interpretation. We propose a new model to explain the thinning of the continental crust beneath the *Mauléon* hyper-thinned rift basin, taking into account the sedimentary evolution of the basin through Cretaceous.

2. Geological setting

Present day structure of the western *Pyrenees*

The Pyrenean mountain belt results from a north-south convergence and collision between Iberian and European continental blocks from the Late Santonian to the Early Miocene

(Puigdefàbregas and Souquet, 1986; Olivet, 1996; Rosenbaum et al., 2002; Sibuet et al., 2004; Gong et al., 2008). The deformation of this intracontinental domain is linked to the northward migration of the Iberian plate and to inversion of the previous Cretaceous north-Pyrenean basin (Ducasse and Vélasque, 1988). The central and eastern parts of the *Pyrenees* can be divided into three structural zones: the North-Pyrenean Zone (NPZ), the *Axial Zone,* and the South-Pyrenean Zone (SPZ) (Fig. 1A; Choukroune, 1976). The NPZ – located between two major faults, the North Pyrenean Fault (NPF) to the south, and the North Pyrenean Frontal Thrust (NPFT) to the north (Fig. 1B; Choukroune and ECORS Team, 1989; Daignières et al., 1994) – is composed of folded Mesozoic cover and Paleozoic units. The commonly named Metamorphic Internal Zone (MIZ), along the southern part of the NPZ, corresponds to a narrow, east-west, vertically metamorphosed and severely deformed zone (Ravier, 1957). The MIZ is characterized by high-temperature and low-pressure metamorphism related to Albian-Cenomanian rifting (Albarède and Michard-Vitrac, 1978; Montigny et al., 1986; Golberg and Maluski, 1988; Golberg and Leyreloup, 1990; Boulvais et al., 2006; Clerc et al., 2015).

In the western *Pyrenees*, the NPZ is represented by the Cretaceous *Mauléon* Basin, thrusted to the north onto the *Aquitaine* Basin and bordered to the south by the *Axial Zone,* where Paleozoic rocks are unconformably overlain by Late Cretaceous shallow marine carbonates (Souquet, 1967). The *Mauléon* Basin is bounded to the west by Paleozoic blocks commonly known as the "*Massifs Basques*" (Heddebaut, 1973; Muller and Roger, 1977). The MIZ and the NPF disappear in the western part of the *Pyrenees* (Choukroune, 1976; Hall and Johnson, 1986; Canérot et al., 2004). The compressive phase is responsible for a greater shortening rate in the central and eastern *Pyrenees* (Muñoz, 1992; Vergés et al., 1995; Beaumont et al., 2000; Mouthereau et al., 2014) than in the western *Pyrenees* (Teixell, 1996, 1998), inducing better preservation of the *Mauléon* Basin. The minor deformation of the western NPZ is linked to diachronism at onset of the thrusting of the Pyrenean compressive phase, older to the east

(Santonian) and younger to the west (Middle Eocene), due to Iberian plate kinematics (Souquet et al., 1977; Séguret and Daignières, 1986; Olivet, 1996). This diachronism is the result of the configuration of the plates before convergence, with a more stretched domain in the western *Pyrenees*. The MIZ re-appears in the commonly named “Nappes des Marbres” corresponding to the center of the Albian basco-cantabric basin (Rat et al., 1983).

The *Mauléon* Basin

The *Mauléon* Basin corresponds to a Cretaceous subsiding domain, filled by thick Albian to Upper Cretaceous deep basin deposits. The *Mendibelza-Igountze* southern Unit correspond to the inverted elements of the paleo-southern *Mauléon* Basin margin (Muller and Roger, 1977; Canérot et al., 1978; Puigdefàbregas and Souquet, 1986). This unit is composed of a Devonian-Carboniferous sedimentary substratum (Laverdière, 1930; Paris, 1964; Casteras et al., 1967; Mirouse, 1967), and a thick Albian synrift *Mendibelza* Formation (Lamare, 1946). The *Mendibelza-Igountze* Unit is thrusted towards the south onto the *Larrau-Saint Engrâce* Triassic window (Galharague, 1966) and the Late Cretaceous carbonate cover of the *Axial Zone*, along the *Lakhoura* Thrust (Lamare 1941; Casteras 1943; Ducasse *et al.* 1986; Teixell 1993).

The *Arbailles* Unit is separated from the *Mendibelza* Unit by the steeply dipping *Arbailles* Thrust (Lamare, 1948), also called the "Licq Fault" (Teixell et al., 2016). The Arbailles Unit is characterized by a preserved Jurassic-Lower Cretaceous carbonate sequence folded in a N110° trending syncline. This syncline is bounded to the north by a major normal fault separating it from the *Saint-Palais* Unit. This latter is represented by a thick (~ 6,000 m) Albian to Late Cretaceous flysch sequence deformed in N110° trending folds of various wave lengths. The north-eastern part of this unit is affected by the *Saint-Palais*, *Bellevue* and *Sainte-Suzanne* (NPFT) northward Pyrenean thrusts (Daignières et al., 1994; Teixell, 1998).

During Cretaceous time, the *Mauléon* Basin is separated from the *Aquitaine* Basin by the "*Grand-Rieu"* Ridge (Serrano et al., 2006).

The *Labourd* and *Aldudes* Units are composed of an Ordovician to Carboniferous sedimentary basement (Laverdière, 1930; Lamare, 1944; Heddebaut, 1967, 1973), overlain respectively by Permian-Triassic continental deposits (Lucas, 1985) and an Upper Cretaceous carbonate platform (Souquet, 1967). The *Labourd-Aldudes* N20° Units, forming the western margin of the *Mauléon* rift Basin (Fig. 2), coincide with the commonly named *Pamplona* Fault identified by the authors Richard, 1986; Razin, 1989; Claude, 1990; Larrasoaña et al., 2003; Pedreira et al., 2007. The northern part of the *Labourd* Unit is composed of the *Ursuya* granulites (Viennot and Kieh, 1928; Lamare, 1939; Boissonnas et al., 1974; Hart et al., 2016).

The eastern part of the *Mauléon* Basin is materialized by the "*Chaînons Béarnais*", corresponding to a N110° anticline and syncline system, affecting a Jurassic to Early Cretaceous carbonate cover (Canérot, 1988). This sedimentary cover is associated with lherzolite outcrops: "*Urdach*, *Tos de la Coustette*, *Saraillé*, *Turon de la Técouère*" (Fabriès et al., 1991, 1998). The *Urdach* mantle body is reworked into Late Albian to Cenomanian synrift breccias, composed of Paleozoic basement and mantle clasts (Roux, 1983; Fortané et al., 1986; Jammes et al., 2009; Debroas et al., 2010; Lagabrielle et al., 2010).

Tectono-sedimentary evolution of the *Mauléon* Basin

The Permian-Triassic post-Hercynian continental deposits filled extensional basins, such as the *Bidarray* Basin (Fig. 2), located in the *Labourd-Aldudes* Units (Bixel and Lucas, 1983, 1987). The Late Triassic deposits are characterized by a Lower Triassic Sandstone Unit, a Middle Triassic Carbonate Unit and an Upper Triassic shale, evaporite and ophite complex (Curnelle, 1983; Lucas, 1985; Rossi et al., 2003). During the Jurassic, a carbonate platform developed in a relatively stable tectonic context (Delfaud and Henry, 1967; Lenoble, 1992;

James, 1998). The end of the Jurassic is characterized by large scale exposure of the Aquitain-Pyrenean domain. The Neocomian is lacking on this part of Pyrenees and is recorded by the development of the bauxites (Combes et al., 1998; James, 1998; Canérot., 2008). During Early Barremian, localized subsidence of the previously emerged domain favored the transgression of carbonate platform deposits that continued until the earliest Albian (Delfaud and Villanova, 1967; Arnaud-Vanneau et al., 1979). The end of this period is marked locally by extensive halokinetic deformation, associated with the first normal faults and the development of distal spicules marls (Canérot, 1988, 1989; Canérot and Lenoble, 1993; James and Canérot, 1999; Canérot et al., 2005).

The deposition of a thick, deep-marine conglomeratic sequence on the southern margin (*Mendibelza-Igountze* Unit) of the newly formed *Mauléon* Basin is considered as marking the onset of the Albian rifting basin, with a strong differentiation between an uplifted southern domain being the source of the conglomerates and a strongly subsiding deep-marine basin to the north (Boirie, 1981; Boirie and Souquet, 1982; Fixari, 1984; Souquet et al., 1985; Fig. 2). In the basin axis, more distal turbidites of the Black Flysch group, time-equivalent to the *Mendibelza* Conglomerates on the southern margin, constitute the first stratigraphic unit of the North-Pyrenean rift. At the same time, along the more gently-dipping northern margin, the albian shallow-marine carbonate deposits grade southwards to more distal marl-dominated sedimentation (Biteau et al., 2006).

The *Mauléon* Basin widened during the Cenomanian to Santonian (Canérot, 2017). Active carbonate turbiditic systems supplied by the Aquitain platform to the north are responsible for the deposition of a thick carbonate flysch sequence at the basin axis (Razin, 1989). At the southern margin, the transgressive "*Calcaires des Cañons*" carbonate platform onlaps the previously emerged Paleozoic basement, currently exposed in the *Axial Zone* (Casteras and Souquet, 1964; Souquet, 1967; Alhamawi, 1992). Chaotic gravity-flow sedimentation

characterized the southern tectonically-controlled erosional slope (Durand-Wackenheim et al., 1981). From Late Santonian to Eocene times, a thick deep-water sequence deriving from eastern syn-tectonic siliciclastic systems accumulated in the *Mauléon* Basin. Finally, the basin was deformed and inverted by the Pyrenean compression from the Middle Eocene to the Miocene (Puigdefàbregas and Souquet, 1986; Bosch et al., 2016; Labaume et al., 2016).

Present day deep structure of the *Mauléon* Basin

Gravimetric studies highlight a strong positive gravity anomaly under the *Mauléon* Basin (Grandjean, 1992, 1994; Casas et al., 1997). This was previously considered as a dense intra-crustal anomaly (Grandjean, 1994) but is now interpreted, by some authors, as being induced by the proximity of the lithospheric mantle below a thinned crust (Wang et al., 2016; Wang, 2017). Recent research efforts focusing on mantle exhumation have linked denudation of the "*Chaînons Béarnais*" mantle outcrops to Albian hyper-thinning crustal mechanisms along a low angle detachment fault (Jammes *et al*. 2009; Lagabrielle *et al*. 2010; Masini *et al*. 2014; Tugend *et al*. 2014; Corre *et al*. 2016; Teixell *et al*. 2016). The inversion of this rift basin is responsible for the Iberian northward underplating (Mattauer, 1985; Engeser and Schwentke, 1986; McCaig, 1988; Choukroune et al., 1990).

Available geodynamic models of the *Mauléon* rift basin

The crustal thinning process of the *Mauléon* rift basin during Albian times has been debated recently (Jammes et al., 2009; Masini et al., 2014; Tugend et al., 2014, 2015a; Corre et al., 2016; Teixell et al., 2016; Fig. 3). Rifting reconstructions differ from crustal thinning models, salt tectonics and synrift filling geometries. The first models describe this basin as a classical rift, thinned by basinward-dipping, crustal, normal faults, responsible for the development of tilted blocks on the southern margin of the rift (Boirie and Souquet, 1982; Fixari, 1984; Souquet et al., 1985; Canérot and Delavaux, 1986; Canérot, 1988; Ducasse and Vélasque,

1988; Souquet, 1988). In recent models of crustal hyper-thinning processes, sub-continental mantle exhumation is interpreted as being related to northward-dipping detachment faults in the distal part of the basin (Jammes *et al*. 2009; Tugend *et al*. 2014, 2015a; Masini *et al*. 2014; Fig 3A). According to these models, the southern margin of the *Mauléon* Basin corresponds to the "lower plate" and the northern *Grand-Rieu* Ridge to the "upper plate" (sensu Wernicke, 1985; Lister et al., 1986). The *Ursuya* granulites are also considered as lower to middle crust exhumed during this Albian extensional stage. Two extensional fault systems, the north and south *Mauléon* detachments, could be responsible for the southward tilting of the *Mendibelza* and *Arbailles* Units (Masini et al., 2014). An alternative model suggests that the Albian thinning of the continental crust was caused by a process of crustal boudinage and led to the creation of a symmetric basin and sliding of the Mesozoic cover from the margins towards the basin axis on each margin (Lagabrielle et al., 2010; Corre et al., 2016; Teixell et al., 2016; Fig. 3B).

Our working approach was to reconstruct a N-S cross-section of the present-day *Mauléon* Basin, using a field approach on the southern margin and seismic data to illustrate the northern one. The Albian reconstitution of this cross-section allows to consider the tectono-sedimentary evolution of the basin, focusing on the Albian-Cenomanian rifting phase. The first part of this paper focuses on a description of the southern margin of the *Mauléon* rift basin based on outcrop data. The second part focuses on the deep geometry of the *Mauléon* Basin, using the interpretation of a N-S reprocessed composite seismic reflection profile. This line shows the deep geometry of the conjugate rift margins. The third part of the paper presents a new N-S composite crustal section of the entire *Mauléon* Basin, and a reconstitution at Cenomanian time. We propose a new model of crustal thinning highlighting the individualization of the Iberian and European conjugate rift margins.

3. The southern margin of the *Mauléon* Basin from field observations

Field work has enabled updating of the 1/ 50 000 BRGM geological maps. The latter image the Iberian margin of the *Mauléon* Basin: (1) *Mendibelza Unit*; and (2) *Arbailles Unit* (Fig. 4A). The southern margin of the *Mauléon* Basin was deformed during the Eocene alpine compression along several southward-verging thrusts. The most significant of these, known as the *Lakhoura* Thrust, is responsible for the under-thrusting of the *Axial Zone* beneath the North-Pyrenean units (Fig. 4). Five structural units bounded by tectonic contacts have been defined from south to north on this inverted margin (Fig. 4B): (1) The *Axial Zone,* formed by the Paleozoic basement and its Late Cretaceous cover (over-thrust by the northern units along the *Lakhoura* Thrust); (2) The *Saint-Engrâce/Bedous* Unit, composed of a complex assemblage of Triassic rocks thrusted onto the *Axial Zone* to the south; (3) The *Mendibelza-Igountze* Unit, including Albian deep-marine synrift deposits onlapping the Paleozoic sedimentary basement (Fig. 5); (4) The *Arbailles* Unit, represented by carboniferous rocks overlain by a continental to shallow marine Triassic to earliest Albian sequence; and (5) the *Saint-Palais* Unit formed, essentially, of a thick Albian to Late Cretaceous turbiditic sequence overlying a deformed Jurassic to Early Cretaceous Carbonate unit.

The *Axial Zone*

The Palaeozoic basement of the *Axial Zone* is stratigraphically covered by a shallow marine carbonate sequence, Cenomanian to Santonian in age, known as the "*Calcaires des Cañons*" (Souquet, 1967; Fig. 6A). This carbonate platform succession is overlain by deeper Late Santonian to Maastrichtian marine sediments composed of argillaceous mudstone ("calcshists") containing planktonic foraminifera, grading upward and laterally to siliciclastic deposits. This deep marine depositional setting continues at least until the Early Lutetian in this domain. The Paleozoic rocks are not greatly deformed near the contact with the Late Cretaceous carbonates (*Ehujarré* and *Kakoueta* areas).

The *Saint-Engrâce – Bedous* Unit

This unit has extensive eastward continuity (*Aspe* Valley), justifying its name *Bedous*. The *Saint-Engrâce-Bedous* Unit observed in the *Larrau* tectonic window is a discontinuous thin band of Triassic rocks delimited by two thrusts and squeezed between the *Axial Zone* to the south and the *Mendibelza – Igountze* Unit to the north (Ducasse and Vélasque, 1988; Teixell, 1993). The *Saint-Engrâce-Bedous* Unit is composed of the Middle Triassic Carbonate Unit and the Upper Triassic shale, evaporite and ophite complex. These Triassic rocks are affected by EW-trending folds indicating a southward displacement of the *Lakhoura* Thrust system.

The *Mendibelza-Igountze* Unit: contacts between the Paleozoic basement and the synrift deposits

The *Mendibelza-Igountze* Unit is composed of Albian deep-marine synrift deposits onlapping the Paleozoic sedimentary basement. The *Mendibelza* synrift conglomeratic gravity flow deposits have already been studied, by the following authors: Fournier 1905, 1908; Lamare 1939, 1946, 1948; Gubler *et al*. 1947; Magné 1948; Viers 1956; Paris 1964; Poignant 1965; Galharague 1966; Merle 1974, Boirie 1981; Fixari 1984; Souquet *et al*. 1985. The Palaeozoic substratum of the *Mendibelza* Formation (Fm.) is composed of Late Devonian to Carboniferous sedimentary rocks (Fig. 5). This substratum is exposed at two highs: the *Esterençuby* high to the north and the *Occabe* high to the south. The Albian conglomeratic *Mendibelza* Fm. is very thick (2,000 m; Fig. 6A) at the northern block, much thinner at the southern one. The pebbles in this conglomerates are made up of Paleozoic sedimentary basement and Early Albian carbonate platform in the *Igountze* area (“Floridées limestones”). In this area, the base of this conglomeratic sequence is composed of discontinuous calci-turbidites reworking the Early Albian carbonate platform and the Paleozoic basement. In the *Mendibelza* area, the base of this formation is characterized by discontinuous base-of-slope

sedimentary breccias reworking the Lower Triassic Sandstone Unit (Figs. 7A and B). These discontinuous *Igountze* calci-turbidites and *Mendibelza* breccias materialized the base of the *Mendibelza* Formation, that is overlied by three southward back-stepping mega-sequences defined by Souquet et al., 1985. The *Mendibelza* conglomerates are overlain by Cenomanian to Santonian polymictic chaotic breccias reworking the "Calcaires des Cañons" carbonate platform of the *Axial Zone* and angular blocks of the Paleozoic sedimentary basement. These deposits attest a base-of-slope palaeogeographic boundary between the *Axial Zone* and the *Mendibelza-Igountze* Unit during the Late Cretaceous. Along the N-S geological cross-section (Fig. 4), the *Mendibelza-Igountze* Unit is overthrust southward by the *Lakhoura* Thrust, onto the *Axial Zone* and the *Saint-Engrâce* Unit. The *Mendibelza-Igountze* Unit is also thrusted towards the west, onto the *Aldudes* Unit. The Cretaceous to Paleocene synrift and post-rift strata are affected by the *Lakhoura* Thrust, as shown by their vertical to overturned position along the front of the *Lakhoura* Thrust on the southern limit of the *Mendibelza* Unit, indicating that this thrust is post Cretaceous.

First rift models described the *Mendibelza-Igountze* Unit as turbiditic proximal cones installed on the southward tilted blocks affecting the Iberian margin of the *Mauléon* Albian Basin (Boirie and Souquet, 1982; Fixari, 1984; Souquet et al., 1985; Canérot and Delavaux, 1986; Canérot, 1988; Ducasse and Vélasque, 1988; Souquet, 1988). However, in the light of recent understanding of crustal hyper-thinning processes, Masini *et al*. (2014) have interpreted the southward tilting of the *Mendibelza-Arbailles* Unit as resulting from the development of a northward detachment fault. To evaluate these different hypotheses, a detailed field analysis was conducted to determine the nature of the substratum / cover contacts and the synrift deposit geometry. All the contacts observed in the field between the substratum and the synrift deposits are primary contacts that were not reactivated during the Pyrenean orogeny. Two kinds of contacts have been distinguished: (1) depositional surfaces; and (2) syn-

295 sedimentary faults. All these surfaces have been corrected for post-depositional tilting in order
296 to reconstruct their geometries at the time of the syn-rift deposition (Fig. 8).

297 Albian depositional surfaces

298 The depositional surfaces (yellow and blue lines in Fig. 5) are in all cases characterized by an
299 angular unconformity with the Albian synrift strata. This unconformity is between 15–40°
300 (Fig. 8). Our facies analysis of the *Mendibelza* Fm. confirms that this unit consists of
301 conglomeratic gravity-flow deposits (Boirie, 1981; Boirie and Souquet, 1982; Fixari, 1984;
302 Souquet et al., 1985). The composition, the very coarse granulometry and the roundness of the
303 clasts suggest that this base-of-slope gravity system was fed by non-preserved shelf-edge fan-
304 deltas, reworking the Paleozoic meta-sedimentary units in an uplifted southern area located in
305 the present day *Axial Zone*. In this context, these deep marine conglomerates are considered to
306 have been deposited in a close to horizontal position. In addition, the *Mendibelza* Fm. is
307 currently stacked with an average regional dip of N120°–30 to 40°SW, without any wedge-
308 shaped syn-tectonic growth strata. These characteristics make it possible to reconstruct the
309 inclination of the depositional surfaces of the synrift albian deposits on the Palaeozoic
310 substratum (Fig. 8). The surfaces are generally tilted from 15° to 40° towards the NE to NNE,
311 with an average value of 30°, once the *Mendibelza* Fm. strata have been reseated in the
312 original horizontal position. This shows that the Albian substratum of the proximal part of the
313 *Mauléon* Basin was inclined towards the basin axis at the time of the synrift *Mendibelza* Fm.
314 deposition. Locally, the *Esterençuby* high is characterized by an albian surface inclined at 30°
315 to 50° towards the east.

316 Albian synsedimentary vertical normal faults

317 Two fault systems have been identified: (1) the N110°–45°NNE North *Occabe* Fault (NOF, in
318 orange in Figs. 5 and 8); and (2) the N20° vertical normal *Esterençuby* faults (in purple in Fig.

5). These faults have an angular relationship of between 75° and 90° with the strata of *Mendibelza* conglomerates. Reconstruction of these faults indicates an original orientation and dip of N120°–75 to 85° NE for the NOF and an unchanged N20° vertical for the *Esterençuby* faults. The Early-Middle Albian megasequences 1 and 2 of the Black Flysch (Souquet et al., 1985) were deposited during the activity of the NOF which is sealed by the upper part of megasequence 2 (Fig. 5). The stratal geometries and geological mapping show that the activity of the N20° *Esterençuby* fault system was contemporary with the NOF, i.e. during the Early-Middle Albian.

Megasequence 3 onlapped the *Occabe* high during the Late Albian. The occurrence of chaotic gravity flow deposits from the Late Albian to Santonian, on the Occabe domain implies the presence of a tectonically controlled scarp in between the emerged to shallow marine Axial Zone and the deep marine Mendibelza domain. However this fault scarp is now overprinted by the Lakhoura Thrust. Therefore, these faults are diachronous and increasingly younger towards the southern margin of the *Mauléon* Basin, since the North *Occabe* Fault is sealed by Middle Albian deposits. These observations are in agreement with the southward back-stepping of the Albian deposits (Souquet et al., 1985).

The Palaeozoic rocks are affected locally by low temperature weak deformations (Fig. 7C). But several of these cataclasites are sealed by Permian sediments indicating a Late-Hercynian age for this deformation (Fig. 5). These observations do not therefore confirm the occurrence of cataclasites punctuating a detachment fault between the Hercynian basement and the Albian synrift deposits, as proposed by Jammes et al. (2009), Masini et al. (2014).

The *Mendibelza* Unit: preliminary interpretations

Most previous publications describe the *Mendibelza* Unit as an Early Albian southward tilted block, characterized by a stratigraphic or tectonic contact between the substratum and the

Albian *Mendibelza* conglomerates (Ducasse *et al*. 1986; Souquet *et al*. 1985; Ducasse & Vélasque 1988; Souquet 1988; Masini *et al*. 2014). However, the present study, based on field analysis and structural reconstruction, does not support these interpretations. Quite the opposite in fact: it shows an absence of wedge-shaped syn-tectonic growth strata in the Albian synrift sequence and depositional surface on the hercynian substratum inclined from 15 to 40° towards the NE. The hercynian substratum of the *Mendibelza* Unit dips towards the *Mauléon* Basin axis. The tilt of this unit towards the NE is marked by the development of diachronous N120° normal faults that are increasingly younger towards the south. The present day tilting of the Albian sequence, about 45° towards the south, postdates the *Mendibelza* Formation.

The *Arbailles* Unit: tectonic and stratigraphic framework

The contact between the *Arbailles* and the *Mendibelza* Units corresponds currently to a vertical fault. Due to the overturned and northward-dipping position of the Albian sequence of the *Mendibelza* Unit to the south, this fault is interpreted as a verticalized southward-directed thrust fault called the *Arbailles* Thrust (Ducasse and Vélasque, 1988, Fig. 4). This thrust is locally retro-thrusting towards the north, indicating a later northward displacement of the *Mendibelza* Unit responsible for the verticalization of the previous *Arbailles* Thrust (Dumont et al., 2015). The *Arbailles* Unit is bounded northward by a set of northward-dipping to sub-vertical normal faults, known as the North *Arbailles* Fault (NAF, Fig. 9). These N120° faults result in a juxtaposition of Barremian - Aptian shallow-marine carbonate deposits to the south, and deeper marine marl-dominated Albian deposits to the north. This set of faults disappears eastward. In fact, the *Arbailles* Unit is overlapped eastward by the Albian-Cenomanian *Tardets* Black Flysch group deposits (Souquet et al., 1985). Westward, the *Arbailles* Unit is bounded by the *Saint-Jean-Pied-de-Port* Upper Triassic Unit.

366 The *Arbailles* Unit consists of a carboniferous basement, a Late Triassic sequence and a
367 Mesozoic cover (Figs. 4 and 9). In this sector, the Late Triassic shales and evaporites overlie
368 the Lower Triassic sandstone unit, without any Middle Triassic carbonate Unit. The Upper
369 Triassic Unit is widely exposed on the south-west and consists of ophites and numerous
370 cargneules indicating a wide zone of deformation. There is a classical Jurassic sequence
371 above the Upper Triassic Unit (Lenoble, 1992). This Jurassic sequence is limited at the top by
372 an erosional surface marked by greater and greater truncation towards the south-west,
373 explaining the lack of most of the Late Jurassic in the southern part of the *Arbailles* Unit (Fig.
374 6A). This unconformity is linked to the Late Jurassic - Early Cretaceous emersion phase,
375 associated regionally with the development of bauxites (Combes et al., 1998; James, 1998;
376 Canérot et al., 1999). The geometry of this surface reflects the tilt of the Jurassic deposits
377 towards the north during this period. This emersion extends as far as the base of the
378 Barremian, as evidenced by the lack of Neocomian deposits in the *Arbailles* Unit (Fig. 6A).

379 The Barremian to earliest Albian carbonate platform deposits onlap the Jurassic carbonate
380 platform towards the south-west (Fig. 6A). This onlapping is highlighted by the southward
381 thinning of the Barremian deposits and the interbedding of transgressive conglomerates
382 including pebbles reworked from the pre-existing Kimmeridgian carbonates (Fig. 7D). The
383 Aptian carbonates (Urgonian facies) overlying the Barremian to the north backstep towards
384 the south and onlap the eroded Jurassic sequence directly in this direction. The thickness of
385 the Aptian deposits increases northward without significant facies change, indicating a
386 northward increase in subsidence (towards basin axis, Figs. 4, 6A and 9).

387 From Late Aptian to earliest Albian, algal carbonates ("Mélobésiées" limestone) onlap the
388 eroded Jurassic sequence in the southern part of the *Arbailles* Unit (Fig. 7E). Intraformational
389 breccias (Fig. 7F) attest to the presence at that time of an unstable depositional setting and
390 probably a slight inclination of the depositional profile. This is confirmed by the northward

change in facies from shallow marine carbonates to deeper marine spicule marls with intercalations of some carbonate debrites towards the north (Fig. 7G and H). This Late Aptian-Early Albian sequence is affected by two kinds of progressive unconformity: (1) a generalized and progressive northward thickening of this sequence at the scale of the *Arbailles* Unit, linked to a northward increase in the subsidence rate; and (2) a growth strata unconformity of shorter wavelength that could result from diapiric movements along the southern edge of the *Arbailles* Unit (Canérot, 1988, 1989, 2008; Canérot and Lenoble, 1993).

The *Saint-Palais* Unit

The *Saint-Palais* Unit is located between the *Arbailles* Unit and the *Saint-Palais* Thrust. The *Saint-Palais* Unit formed the Albian - Late Cretaceous depocenter of the *Mauléon* Basin. At outcrop scale, this unit is folded into N120° synclines / anticlines of pluri-kilometric wavelength, composed of Early Albian spicule marls and Middle Cenomanian - Turonian carbonate distal turbidites. The northern part of this unit is affected by the N110-120° overturned *Saint-Palais* anticline. Field work confirms that the distal Late Cretaceous carbonate turbidites are sourced from the north by the European carbonate platform, as shown by the N150–200° directed paleocurents measured in the field. These Late Cretaceous carbonate deposits overlaid the Albian sequence unconformably. This is shown by the southward distal onlap of the Late Cretaceous deposits on the Albian synrift sequence, on the southern edge of the *Saint-Palais* Unit.

4. Seismic interpretation of the *Mauléon* Basin and the southern part of the *Aquitain* Basin

Unlike the southern margin that has been observed directly in the field (*Mendibelza* and *Arbailles* Units), the architecture of the central part and the northern conjugate margin of the

414 *Mauléon* Basin have been explored from seismic data and well calibration (Figs. 6 and 10).
415 This section focuses on the deep geometry of the *Mauléon* Basin from the interpretation of a
416 N-S composite seismic reflection profile, reprocessed by the BRGM in 2017 (MT104 and
417 MT112 acquired by ESSO-Rep in 1969 on the *Mauléon-Tardets* exploration permit, ***cf 4.2***).
418 The seismic line interpreted is a merger of lines MT104, MT112 and 83HBS02 (acquired by
419 SNEAP in 1981 and reprocessed by BRGM in 2014; Fig. 10). The seismic interpretation was
420 carried out using the Geographix® Discovery Suite that allows for each CDP of the seismic
421 profile to export its X, Y, time, amplitude and depth values. Seismic/well tie is obtained by
422 using the time / depth curves acquired in the boreholes and derived from the recording of
423 checkshots. The time / depth conversion was performed using a mean velocity field calculated
424 on the basis of all the time / depth data of the calibration wells, integrating their deviations
425 (Fig. 11). The top basement has been calibrated taking into account the ECORS seismic
426 reflection profile (Daignières et al., 1994). The composite line presented in this paper is
427 calibrated with six wells (Fig. 6), from south to north: *Ainhice*-1 (3,540.85 m depth); *Uhart-*
428 *Mixe*-1 (1,868.8 m depth); *Bellevue*-1 (6,909 m depth); *Orthez*-102 (5,489.10 m depth);
429 *Amou*-1 (5,543 m depth); and *Bastennes-Gaujacq*-1.bis (4,442.10 m depth). Only the *Ainhice*-
430 1 well reaches the Paleozoic basement of the *Mauléon* Basin. The studied SSW-NNE seismic
431 line through the *Mauléon* Basin cuts across four distinct structural units, separated from one
432 another by thrust faults (Fig. 10). From south to north, the units are as follows: (1) *Saint-*
433 *Palais;* (2) *Bellevue;* (3) *Sainte-Suzanne;* and (4) Grand-Rieu/*Arzacq* (Figs. 6 and 10). The
434 *Saint-Palais* Unit corresponds to the central and deepest part of *Mauléon* Basin, while the
435 *Bellevue* and *Sainte Suzanne* Units belong to its northern margin. The *Bellevue* and *Sainte*
436 *Suzanne* thrusts involved the European basement. Using the field cross-section (Fig. 4B) and
437 well-velocity models calibrating the interpreted composite seismic reflection profile (Fig. 10),
438 we propose a depth migrated section of the entire Mauléon Basin (Fig. 11).

The *Saint-Palais* Unit

The Palaeozoic substratum below the *Saint-Palais* Unit is tilted towards the north, being at a depth of around 2,900 m in the *Ainhice*-1 well (Fig. 6) and of 7,000 m in the central part of the basin. The base of this well is characterized by Paleozoic basement, overlain by the thick Upper Triassic salt Unit materializing a major decoupling level between the basement and the sedimentary cover. This Triassic salt unit is grading upward to two Mesozoic cover units characterized by a normal polarity and separated by a tectonic contact. The Lower Unit, U1, consists of a complete Jurassic sequence, up to the Kimmeridgian, covered by Late Aptian Urgonian limestones. Unit U1 is characterized by a hiatus of the Neocomian to the Early Aptian. The Upper Unit, U2, is composed of the same Jurassic but the Kimmeridgian marls are thinner than in U1, grading upward to Earliest Albian carbonate platform deposits (Fig. 6A). These cover units are overlain by Middle to Late Albian spicule marls and siliciclastic turbidites. The Albian basinal deposits thicken towards the north and reach their maximum thickness in the *Saint-Palais* Anticline, clearly identified in the field. The *Saint-Palais* domain corresponds to the depocenter of the Albian basin, with an estimated thickness of up to 4,000–5,000 m (Roux, 1983; Fixari, 1984; Souquet et al., 1985). The upper part of the *Saint-Palais* Unit is formed by the Upper Cretaceous carbonate-dominated flysch, which reaches a thickness of more than 1,500 m in the *Uhart Mixe* well.

The *Bellevue* Unit

The *Bellevue* Unit is located between the *Saint-Palais* and the *Bellevue* Thrusts. The *Bellevue* Thrust is responsible for the offset of the Jurassic-Cretaceous cover and the displacement of the *Bellevue* Unit onto the *Sainte Suzanne* Unit. The Paleozoic basement is located at a depth of around 8,000 m under the Bellevue Unit. This unit is composed of a complex structure whose most obvious feature is the Bellevue Anticline affecting the Mesozoic cover

intersected in the *Bellevue* well. The northward *Bellevue* Thrust is marked by a 1,800 m thick tectonized zone composed of Late Triassic salt and Barremian carbonate slices. These Barremian units could be tectonically incorporated to the Triassic salt forming the overturned flank of the overlying anticline evidenced in the *Bellevue* well (Fig. 6). In fact, this tectonized interval is overlain by an overturned Jurassic carbonate unit composed of Dogger to Kimmeridgian deposits. Above, the *Bellevue* Unit is made up of a complete Jurassic to Late Cretaceous sequence in a normal position. The Early cretaceous sequence is characterized by a lack of Neocomian. The Barremian to Aptian carbonate platform unit lying unconformably on the Portlandian is more than 1,500 m thick. The Barremian deposits are composed of limestones with annelids and 500 m thick of more distal *Sainte-Suzanne* marls. The Aptian is mainly composed of Urgonian limestones. The Albian thins towards the North and is represented by spicule marls including intercalations of carbonate mudstone indicating the proximity of the northern *Aquitanian* carbonate platform. The Late Cretaceous sequence is made up of Cenomanian to Coniacian carbonate turbidites.

The *Sainte-Suzanne* Unit

The *Sainte-Suzanne* Thrust corresponds to the major north verging thrust responsible for a displacement of more than 17 km of the *Mauléon* Basin deposits onto the south *Aquitain Grand Rieu* Unit (Fig. 10). It can be considered as the North-Pyrenean Frontal Thrust in this part of the *Pyrenees*. The *Sainte Suzanne* Unit is made up of a very thick Jurassic to Campanian sequence, slightly inclined and thickening towards the south. It has been crosscut by the *Orthez*-102 well where the *Sainte Suzanne* Thrust has been identified at a depth of 4,320 m (Fig. 6). The Jurassic is made up of a complete sequence of marine carbonate platform deposits from Hettangian to Kimmeridgian, truncated under the Early Cretaceous deposits, as evidenced by the north-directed erosional truncations. The 1 000m thick Early Cretaceous sequence is characterized by a lack of Neocomian. The Barremian is characterized

by shallow marine carbonate deposits with annelids showing that this unit is more proximal than the *Bellevue* Unit. The Aptian is sub-isopachous and is composed of shallow marine carbonate platform deposits (Urgonian facies). The Albian deposits are also made up of carbonate platform deposits thickening towards the south. These facies are therefore more proximal than the Albian deposits of the *Bellevue* Unit. A clear truncation of the Albian reflections is seen towards the north, below the Late Cretaceous calcareous flysch. This latter calci-turbidite sequence is thinning and onlapping to the north on top of the eroded Albian sequence.

The *Grand-Rieu/Arzacq* Unit

The *Grand-Rieu – Arzacq* Unit is the footwall of the *Sainte Suzanne* Thrust and corresponds to the southern part of the *Aquitain* Basin. From the seismic data, the Paleozoic basement below the *Sainte Suzanne* Thrust can be estimated to be at a depth of 8,500 m. It is assumed to be overlain by a more or less continuous Triassic Unit. The inferred Liassic Unit present in the *Aquitain* Basin to the north appears to pinch-out southwards against a diapiric structure associated with a normal fault. This Mesozoic tectonic structure marks the boundary between the *Grand-Rieu* Ridge to the South and the commonly named *Arzacq* Basin corresponding to a highly subsiding domain during Albian times. The overlying Middle to Late Jurassic carbonates are more continuous and isopachous. The top of the Jurassic sequence corresponds to a major exposure surface marked by north-directed erosional truncations under the Barremian transgressive carbonate deposits, as indicated in the *Amou* well. This unconformity is time-equivalent to the one describe in the *Arbailles* Unit on the southern margin of the *Mauléon* Basin. During the latest Jurassic and the Neocomian period, the northern margin of the *Mauléon* Basin was tilted towards the south, unlike the southern margin that was tilted towards the north. The Barremian to Aptian sequence of the *Grand-Rieu* Unit is relatively isopachous and consists mainly of shallow marine carbonate platform deposits. The Albian

deposits form a thick unit of fairly deep marine spicule marls indicating a strong subsidence rate of the *Arzacq* Basin, as indicated in the *Amou* and *Bastennes-Gaujacq* (Fig. 6). A large wave-length anticline affects the Jurassic - Albian sequence at the transition between the *Grand-Rieu* Ridge and the *Arzacq* Basin (*Grand-Rieu* Anticline). A major truncation of the folded strata below the Cenomanian carbonate platform deposits attests to the Late-Albian to Early Cenomanian age of this deformation. In the *Grand-Rieu – Arzacq* Unit the Late Cretaceous is represented by sub-isopachous carbonate platform deposits. During the Tertiary, this domain was characterized by a very high subsidence rate, increasing towards the South, as attested by the very thick Tertiary sequence at the front of the *Sainte Suzanne* Thrust. Local southward dipping clinoforms can be observed south of the *Bastennes-Gaujacq* well, probably related to the growth of this diapiric structure. The very great thickness of the Tertiary sequence attests to the strong flexural subsidence of the *Grand-Rieu – Arzacq* Unit but also to the large displacement and uplift of the *Mauléon* Basin along the *Sainte-Suzanne* Thrust, since no Tertiary deposits have been preserved in the *Mauléon* Basin (even if they were deposited over this entire flexure domain). Most of the Tertiary flexural subsidence occurs before the Late Lutetian, as shown by the thickening of the Danian to Lower Ypresian deposits towards the south.

5. Top Jurassic to Cenomanian tectono sedimentary and geodynamic evolution of the *Mauléon* Basin

Latest Jurassic to Neocomian uplift phase

The Jurassic is characterized by an extensive and relatively continuous carbonate platform spreading between the southern *Mauléon* Basin margin (*Arbailles* Unit) and the *Arzacq* Basin (Fig. 12A). At its top, the platform is limited by a major unconformity resulting from an emersive and erosional phase dated from the latest Jurassic to Barremian (Fig. 12B). This

event is evidenced by the development of bauxites and the lack of Neocomian deposits both in the *Pyrenees* and the *Arzacq* Basin (Combes et al., 1998; James, 1998; Canérot et al., 1999). Before the Early Cretaceous transgression, the Jurassic platform is characterized by a synform morphology extending from the southern margin of the *Mauléon* Basin to the *Arzacq* Basin. It is revealed respectively by the south-directed and north-directed erosional truncations affecting the Jurassic in the *Arbailles* and the *Arzacq* Units (Fig. 11). This deformation stage implies the uplift of these domains, corresponding partly to the Early Cretaceous Mauléon Basin edges; while in the meantime, subsidence stops in the synform axis. Mechanism responsible for the uplift of the entire Pyrenean-Aquitaine domain might be related to an asthenosphere upwelling preceding the Early Cretaceous rifting.

Barremian to earliest Albian rifting stage 1: symmetric basin

After the Late Jurassic – Early Cretaceous exposure/weathering stage, onset of transgression leads to the development of an extensive restricted carbonate platform during the Barremian. From Barremian to Aptian time, the balance between carbonate production and creation of available space favors the aggradation of 1 600m thick shallow marine carbonate facies, witnessing a highly subsiding stage controlling a relative-flat depositional profile (Figs. 6 and 12C). This homogeneous subsidence stage evolves during Late Aptian to the earliest Albian. The basin's edges were characterized by the back-stepping of the shallow carbonate platform, while the *Mauléon* and *Arzacq* Basins center are composed of deeper spicule marls. In this domain, creation of available space exceeded the carbonate production, resulting in the relocating of the carbonate factory on the basin's edges. Paleogeography reorganization was thus controlled by the differential subsidence regime responsible for a steeper depositional profile.

As a consequence, during the Barremian - earliest Albian time the *Mauléon* Basin was a symmetric basin, characterized by shallow marine carbonate platforms on each basin edges. The absence of brittle deformation within the upper-crust excludes the application of the pure-shear model developed by McKenzie (1978) to explain the subsidence regime of this basin. A symmetric synrift sag basin with no brittle deformation in the upper crust has been proposed from numerical modeling (Karner et al., 2003). In this model, the subsidence of the basin results from lower crustal ductile thinning favored by decoupling between the upper and lower crusts. We propose that the initiation of the *Mauléon* sag basin results from thinning of the lower crust, without any major deformation of the upper crust. The isostatic response to the lower crustal thinning induces regional sagging and onlapping of the syn-thinning deposits on each side of the basin. The rifting stage 1 can be interpreted as a "ductile crustal pure-shear thinning phase".

Albian rifting stage 2: asymmetric basin

At Albian time, the southern margin of the *Mauléon* Basin was affected by differential vertical movements: (1) uplift of the southern part of the basin; and (2) tectonic subsidence towards the north (Fig. 12E). They are responsible for the onset of the *Mendibelza* deep gravity flow deposits passing distally to the Black Flysch group towards the *Saint-Palais* depocenter (Fig. 12E). At this time, the Iberian margin substratum was characterized by a northward dipping surface with an average slope angle of 15–30° (Fig. 8). This surface was affected by syn-sedimentary albian N120° southward-propagating high-angle normal faults, controlling the destabilization of the fan-delta system into the deep basin (Fig. 12E). These faults were sealed by younger synrift back-stepping deposits of the *Mendibelza* Fm. towards the south.

583 The conglomerates directly overlain the Paleozoic substratum of the *Mendibelza* Unit,
584 indicating the entire Mesozoic lacks (Fig. 5), while it was continuous throughout the
585 Pyrenean-Aquitaine domain. Thus, the Mesozoic cover of this unit need to be subtracted prior
586 to the sedimentation of the Albian synrift *Mendibelza* sequence. It leads to the development of
587 an emerged *Axial Zone* during the rifting stage 2. The sliding level consists of the thick Upper
588 Triassic shale, evaporite and ophite complex systematically brecciated and / or deformed
589 under the prerift cover of the Iberian margin. This mass-sliding is recorded within the
590 Ainhice-1 well Mesozoic cover unit overlap (Units U1 and U2, Fig. 6). The stratigraphic
591 differences between these two Mesozoic cover units, suggest an origin of the upper one from
592 a southern marginal part of the basin where the Jurassic-Cretaceous hiatus is greatest. Thus,
593 the Early Albian *Axial Zone* denudation is linked to the northward mass sliding of the
594 Mesozoic cover towards the *Mauléon* Basin axis in response to the Iberian margin northward
595 tilting (Fig. 12D).

596 At the same period, the European margin of the *Mauléon* Basin recorded less vertical
597 movements and tectonic activity than the southern margin. Unlike the Iberian conjugate
598 margin, this northern domain is not subject to gravitational sliding of the Mesozoic cover.
599 Indeed, no regional uplift and associated coarse-grained alluvial-derived gravity-flow deposits
600 are evidenced in the *Arzacq*, *Sainte-Suzanne* and *Bellevue* Units. The Albian period is mainly
601 represented by a shallow marine carbonate platform recognized in the *Arzacq* and *Sainte-*
602 *Suzanne* Units (Figs. 6 and 13). The slightly southward-dipping depositional profile is
603 responsible for a facies transition between shallow-marine algae limestones and deeper
604 spicule marls in the *Sainte Suzanne* Unit. In *Saint Palais* and *Bellevue* Units, the Jurassic-
605 Aptian sedimentary cover is significantly normally offset, which allows the accumulation of
606 thick deep Albian facies to the south of the *Saint-Palais* Thrust, suggesting that this latter
607 corresponds to a southward dipping Albian normal fault (Figs. 11 and 13). This fault is part of

608 the northern *Mauléon* Albian Basin's margin. The thick interval with very deformed Triassic
609 material intersected at the base of the *Bellevue* well is interpreted as an Albian diapiric ridge
610 developing on the northern edge of the Albian *Mauléon* Basin (Fig. 6).

611 Comparison between the southern and northern margins shows that the *Mauléon* Basin
612 acquired asymmetry during the Early Albian time: (1) deep basin turbiditic deposits on the
613 Iberian margin and (2) carbonate platform on the European one. According to most of the
614 models that consider a simple-shear deformation process to explain the asymmetry of a rift
615 (Wernicke, 1985; Lister et al., 1986), the *Mauléon* Basin's asymmetry is interpreted as
616 resulting from the activation of the southward dipping *Saint-Palais* Detachment during the
617 Early Albian (Fig. 13). Following Lister et al. (1986) the Albian Iberian margin corresponds
618 to the upper plate and the European one to the lower plate. The *Saint-Palais* Detachment
619 might be responsible for the northward Iberian margin tilting, this former being part of a
620 major crustal scale roll-over. The roll-over structure is accommodated by N120° oriented and
621 steeply dipping normal faults that propagate towards the south (i.e. NAF, NOF). They are
622 antithetic to the *Saint-Palais* structure. During Albian time, the width of the *Mauléon* deep
623 basin, measured from platform to platform, was around 50 km.

624 **Late Cretaceous rifting stage 3: apparent symmetric basin**

625 During the Late Cretaceous period, a carbonate platform developed on both edges of the
626 *Mauléon* Basin, and the deep basin became wider (Figs. 6 and 13). Indeed, the width of the
627 *Mauléon* deep basin, measured from platform to platform, was around 100 km wide. The
628 *Grand-Rieu* Ridge represents a major palaeogeographic boundary between the carbonate
629 platform of the European margin and the center of the *Mauléon* Basin (Razin, 1989; Serrano
630 et al., 2006). The transition between the carbonate platform and the basinal carbonate
631 turbidites is governed by a southward dipping normal fault between the *Sainte Suzanne* Unit

and the *Arzacq* Basin. The calcareous flysch deposited in the *Mauléon* Basin was derived mainly by gravity flows coming from the northern *Aquitain* carbonate platform. These calcareous turbidites onlap the previous Albian deposits towards the *Sainte-Suzanne* Unit to the north and the *Saint-Palais* to *Mendibelza* Units to the south (Fig. 13). The development of the *Grand-Rieu* Anticline attests of salt movement at Early Cenomanian time.

On the southern margin the commonly named Late Cretaceous *"Calcaires des Cañons"* carbonate platform deposits lie unconformably over the previously exposed Palaeozoic basement of the *Axial Zone* (Fig. 13). Towards the north, in the *Mendibelza* Unit, base-of-slope chaotic breccias attest of a normal fault-controlled platform-basin transition between the southern carbonate platform developing on the *Axial Zone* and the *Mauléon* Basin (Fig. 13). Several arguments indicate that a second and opposite detachment occurred at Early Cenomanian time: the northward verging *Lakhoura* Detachment (Fig. 13). This syn-sedimentary fault, currently inverted as the *Lakhoura* Thrust (Fig. 5), is interpreted as being responsible for the southward tilting of the *Mendibelza/Arbailles* Units. The Early Cenomanian age of this tilting is attested by: (1) the absence of wedge-shaped syn-tectonic growth strata in the Albian synrift sequence of the *Mendibelza* Unit; (2) the 98 Ma cooling age obtained on the (Hart et al., 2017), responsible for the southward tilt of the Lower Triassic Sandstone Unit in the *Saint-Jean-Pied-de-Port* area (Masini et al., 2014); and (3) the onlap of the Late Cretaceous deposits on the tilted and eroded Albian sequence in the north of the *Arbailles* Unit (Casteras et al., 1971; Ducasse and Vélasque, 1988; Fig. 9). This observation implies that the northern edge of the Arbailles Unit becomes a structural high in the basin during Early Cenomanian. This structural high is fossilized at Santonian time as highlighted by the age of the first deposits passing over it.

6. Discussion and Conclusion

The northwestern Pyrenees present a strong positive gravity anomaly under the *Mauléon* rift Basin (Grandjean, 1994; Casas et al., 1997) resulting from the presence at low depth (~10 km) of lithospheric mantle (Wang et al., 2016). This high mantle body position implies the existence of a very thin continental crust arguing for a hyper-thinning Cretaceous rifting stage. In this work, we assume that the *Saint-Palais* and *Lakhoura* structures affect the lithospheric mantle. They are responsible for the hyper-thinning of the *Mauléon* Basin continental crust. However, this rift basin have not underwent oceanic spreading as classical basins along the Atlantic Ocean (Manatschal., 2004; Péron-Pinvidic et al., 2007; Haupert et al., 2016), or in the Alps fossil margins (Manatschal et al., 2006, Masini et al., 2011, Mohn et al., 2014 et Decarlis et al., 2015). Another significant difference with these classical hyper-extended magma poor margins is the thickness of the syn-thinning deposits in the hyper-extended domain (~ 8 km thick in *Mauléon* Basin vs. less than 1 km thick on the Atlantic and Alps margins). The thick synrift deposits record a complex polyphasic thinning history from Barremian to Early Cenomanian time.

During stage 1, the *Mauléon* Basin is symmetric as evidenced by the development of a carbonate platform on each basin edges. The carbonate production counterbalances the high accommodation, resulting in a near flat sedimentary profile. We interpret the creation of accommodation as a result of ductile thinning of the lower crust, without affecting the upper-crust (Fig. 14A). This thinning stage shares similarity with the crustal scale boudinage process, previously proposed at Albian time (Lagabrielle et al, 2010; Corre et al, 2016; Teixell et al, 2016; Fig. 3B). However, only the lower crust is affected by ductile thinning, favored by the presence of a decoupling level in between the lower and upper crusts. The resulting synrift sag basin morphology is quite similar to the Mesozoic *Columbrets* sag Basin, which does not

present any evidence of deep basin gravitary sedimentary infill (Etheve, 2016 and Etheve et al, 2018).

At Albian time (stage 2), the rift fabric totally changed. The basin was affected by "simple-shear thinning" due to the development of the southward dipping *Saint-Palais* Detachment (Fig. 14B). This crustal thinning phase affected the entire lithosphere, forming an asymmetric rift basin, as previously proposed in the simple-shear models (Jammes *et al*, 2009; Tugend *et al*, 2014, 2015a; Masini *et al*. 2014, Fig. 3A). However, unlike the previous models, the Albian rifting stage initiates with simple shear thinning, without distributed extension in the upper crust (pure shear thinning sensus McKenzie., 1978). Lavier and Manatschal., 2006 have evidenced using numerical modeling that the continental crust was already thin (~20km) when simple shear thinning starts. In the case of the *Mauléon* Basin we propose that the Early Cretaceous stage favors the ductile thinning of the lower crust before beginning the Albian-Cenomanian simple shear thinning stage.

The *Saint-Palais* detachment is responsible for the northward Iberian margin roll-over. This interpretation strongly contrasts with previous models arguing for an Albian southward tilt of the Iberian margin along a northward dipping normal fault (Boirie., 1981; Fixari., 1984; Souquet et al., 1985; Ducasse and Vélasque., 1988) or crustal scale detachments (Jammes et al., 2009; Masini et al., 2014). In this scheme, we propose that rift asymmetry controls the asymmetric sedimentary profile. Actually, the Iberian margin (roll-over) is composed of a proximal turbiditic s.l. system whereas the European one (southward gently-dipping) is characterized by a carbonate platform. Similarly, to the *Columbrets* Basin (Etheve., 2016 and Etheve et al., 2018), the onset of simple shear thinning is synchronous with the basinward prerift cover-sliding along the Late Triassic salt décollement. Such Early Albian gravity tectonics have already been reported all along the Iberian rift margin (Bouquet, 1986; Ducasse et al., 1986; Ducasse and Vélasque, 1988; Lagabrielle et al., 2010; Corre et al., 2016; Teixell

et al., 2016; Fig. 3B). However, one of the major discrepancies with the previous models is the absence of gravitational cover sliding along the European rift margin (Fig. 3B). The sliding of the Mesozoic cover led to local diapirism along the Iberian margin, as shown by the lateral facies variations from shallow carbonate platform to spicule marls around the diapiric structures (Canérot, 1988, 1989; Canérot and Lenoble, 1993; James and Canérot, 1999; Canérot et al., 2005).

The paleogeography of the Early Cretaceous *Mauléon* Basin, derived from the sedimentary record is not compatible with a major strike-slip drift of the Iberian plate as proposed in kinematic reconstructions (Le Pichon et al., 1971; Roest and Srivastava, 1991; Olivet, 1996; Rosenbaum et al., 2002; Sibuet et al., 2004; Gong et al., 2008). We assume that the Iberia sinistral strike-slip motion did occur on a more southward structure (Malod., 1982; Canérot., 2016) developed earlier during Late Jurassic (Tugend et al., 2015b) and / or may have been evenly distributed within the Cretaceous rift system.

At Early Cenomanian time (final stage 3), the southward tilting of the *Mendibelza-Arbailles* Units, – formerly considered as Early Albian (Boirie, 1981; Boirie and Souquet, 1982; Fixari, 1984; Souquet et al., 1985; Ducasse and Vélasque, 1988; Masini et al., 2014) – is induced by the change of detachment vergence and the development of the *Lakhoura* northward dipping Detachment. The Arbailles Unit thus becomes a structural high bordering the southern hyper-thinned *Mauléon* Basin domain. Consequently, we assume that the *Arbailles* Unit becomes a tilted block at Early Cenomanian time.

Therefore, the tectono-sedimentary evolution of the *Mauléon* rift Basin during the stages 2 and 3 is defined by the development of two antithetic and diachronous detachments, i.e. the Albian southward dipping *Saint-Palais* detachment during Stage 2 and the Early Cenomanian northward dipping *Lakhoura* one during Stage 3. The change in detachment vergence between

728 Albian and Cenomanian time can be interpreted as "flip-flop detachment tectonic" (Sauter et
729 al., 2013; Geoffroy et al., 2014; Gillard et al., 2015), highlighting the diachronous shift from
730 upper-plate to lower-plate morphology along a same margin section. This double successive
731 asymmetry is responsible for the apparent final symmetry of this hyper-thinned rift. This work
732 reconciliates the previous rift models, i.e. symmetric (Souquet, 1988; Ducasse and Vélasque,
733 1988), asymmetric (Jammes et al., 2009; Masini et al., 2014; Tugend et al., 2015a, Fig. 3A) or
734 mixed (Lagabrielle et al., 2010; Corre et al., 2016; Teixell et al., 2016, Fig. 3B). The
735 polyphase thinning history is responsible for the hyper-thinning of the continental crust and
736 the development of a relatively narrow hyper-thinned rift domain (Fig. 14C).

737 In three dimensions, the *Mauléon* Basin appears relatively complex and not cylindrical. On
738 our synthetic 2D transect (Fig. 14C), the mantle is systematically overlain by a hyper-thinned
739 crust whereas eastward (*Urdach*), it has been denuded and partly reworked into synrift
740 deposits (Roux, 1983; Duée et al., 1984; Fortané et al., 1986; Debroas et al., 2010; Lagabrielle
741 et al., 2010; Teixell et al., 2016). We consider the *Saint-Palais* Detachment as responsible for
742 the hyper-thinning of the continental crust, while the *Lakhoura* one might be responsible for
743 partial mantle denudation. This is consistent with the *Urdach* mantle/crust contact that display
744 top north-east shear direction (Corre., 2017). Thus, it appears that the basin morphology
745 changes along strike, due to N0°-20° transverse structures such as the *Pamplona* (Richard,
746 1986; Razin, 1989; Claude, 1990; Larrasoaña et al., 2003; Pedreira et al., 2007; Díaz et al.,
747 2012), the *Saint-Jean-Pied-de-Port*, *Saison*, *Barlanès* and *Ossau* structures (Canérot, 2008,
748 2017; Debroas et al., 2010). This N0°-20° structuration seems to clearly control the 3D
749 geometry of the *Saint-Palais* hyper-extended rift domain, and will be the purposed of future
750 investigations.

Acknowledgements

This study was conducted within the framework of the integrated geological Orogen research project (TOTAL, BRGM, and INSU). We are very grateful to the reviewers and to the editor, who contributed to the improvement of this manuscript. We would like to thank the Orogen project managers Sylvain Calassou (Total), Emmanuel Masini (Total), Olivier Vidal (CNRS) and French geological survey - BRGM. We also thank Joseph Canérot for the numerous scientific discussions on the tectono-sedimentary evolution of the Mendibelza and Arbailles Units. The authors thank Geoffrey Bird for the English review.

References:

AGSO and BRGM, 2018, Synthèse géophysique et géologique des Pyrénées - Volume 3 : Cycle alpin : Phénomènes alpins – 2015, Edition AGSO and BRGM, coordinated by A. BARNOLAS (1982-2001), B. GUÉRANGÉ (1982-90) J.C. CHIRON (1991-95) and S. COURBOULEIX (1996-2001), scientific committee : A. AUTRAN, M. DURAND-DELGA and J.M. FONBOTÉ, 480 p., 286 figs.

Albarède, F., and A. Michard-Vitrac, 1978, Age and Significance of the North Pyrenean Metamorphism: Earth and Planetary Science Letters, no. 40, p. 327–332.

Alhamawi, M., 1992, Sédimentologie, Pétrographie Sédimentaire et Diagenèse des Calcaires du Crétacé supérieur de la Marge Ibérique: Bordeaux 1, 356 p.

Arnaud-Vanneau, A., H. Arnaud, J. Charollais, M.-A. Conrad, P. Cotillon, S. Ferry, J.-P. Masse, and B. Peybernès, 1979, Paléogéographie des calcaires urgoniens du sud de la France: Géobios, v. 3, p. 363–383.

Baudin, T., and A. Barnolas, 2008, Carte Géologique des Pyrénées au 1/400000, Orléans, France: Bureau de Recherche Géologique et minière.

Beaumont, C., J. A. Muñoz, J. Hamilton, and P. Fullsack, 2000, Factors controlling the Alpine evolution of the central Pyrenees inferred from a comparison of observations and geodynamical models: Journal of Geophysical Research, v. 105, no. B4, p. 8121–8145.

Biteau, J.-J., A. Le Marrec, M. Le Vot, and J.-M. Masset, 2006, The Aquitaine Basin: Petroleum Geoscience, v. 12, p. 247–273.

Bixel, F., and C. Lucas, 1987, Approche Géodynamique du Permien et du Trias des Pyrénées dans le cadre du sud-ouest européen: Cuadernos Geología Ibérica, v. 11, p. 57–81.

Bixel, F., and C. L. Lucas, 1983, Magmatisme, tectonique et sédimentation dans les fossés stéphano-permiens des Pyrénées occidentales: Revue de géologie dynamique et de géographie physique, v. 24, no. 4, p. 329–342.

Boirie, J.-M., 1981, Etude Sédimentologique des Poudingues de Mendibelza (Pyrénées Atlantiques): Toulouse, Université Paul Sabatier (Sciences), 114 p.

787 Boirie, J.-M., and P. Souquet, 1982, Les poudingues de Mendibelza: dépôts de cônes sous-
788 marins du rift albien des Pyrénées: Bulletin Centres Recherches Exploration-
789 Production Elf-Aquitaine, v. 6, no. 2, p. 405–435.

790 Bois, C., and ECORS Scientific team, 1990, Major geodynamic processes studied from the
791 ECORS deep seismic profiles in France and adjacent areas: Tectonophysics, v. 173,
792 no. 1–4, p. 397–410.

793 Boissonnas, J., G. Le Pochat, C. Thibault, and M. Bernatzk, 1974, Carte géologique de la
794 France au 1/50000; feuille d'Iholdy, Orléans, France: Bureau de Recherche
795 Géologique et minière.

796 Bosch, G. V., A. Teixell, M. Jolivet, P. Labaume, D. Stockli, M. Domènech, and P. Monié,
797 2016, Timing of Eocene–Miocene thrust activity in the Western Axial Zone and
798 Chaînons Béarnais (west-central Pyrenees) revealed by multi-method
799 thermochronology: Comptes Rendus Geoscience, v. 348, no. 3–4, p. 246–256,
800 doi:10.1016/j.crte.2016.01.001.

801 Boulvais, P., P. de Parseval, A. D'Hulst, and P. Paris, 2006, Carbonate alteration associated
802 with talc-chlorite mineralization in the eastern Pyrenees, with emphasis on the St.
803 Barthelemy Massif: Mineralogy and Petrology, v. 88, no. 3–4, p. 499–526,
804 doi:10.1007/s00710-006-0124-x.

805 Bouquet, B., 1986, La bordure mésozoïque orientale du Massif du Labourd (Pyrénées
806 occidentales) : Stratigraphie-Sédimentologie-Structure-Implications Géodynamiques:
807 Pau, Université de Pau et des Pays de l'Adour, 219 p.

808 Brun, J.-P., and J. van den Driessche, 1994, Extensional gneiss domes and detachment fault
809 systems; structure and kinematics: Bulletin de la Société Géologique de France, v.
810 165, no. 6, p. 519–530.

811 Brune, S., C. Heine, M. Pérez-Gussinyé, and S. V. Sobolev, 2014, Rift migration explains
812 continental margin asymmetry and crustal hyper-extension: Nature Communications,
813 v. 5, doi:10.1038/ncomms5014.

814 Brune, S., S. E. Williams, N. P. Butterworth, and R. D. Müller, 2016, Abrupt plate
815 accelerations shape rifted continental margins: Nature, v. 536, no. 7615, p. 201–204,
816 doi:10.1038/nature18319.

817 Canérot, J., 1988, Manifestations de l'halocinèse dans les chaînons béarnais (zone Nord-
818 Pyrénéenne) au Crétacé inférieur: Comptes rendus de l'Académie des sciences Série 2,
819 v. 306, no. 15, p. 1099–1102.

820 Canérot, J., 1989, Rifting éocrétacé et halocinèse sur la marge ibérique des Pyrénées
821 Occidentales (France). Conséquences structurales: Bulletin Centres Recherches
822 Exploration-Production Elf-Aquitaine, v. 13, p. 87–99.

823 Canérot, J., 2008, Les Pyrénées: Histoire géologique: Atlantica.

824 Canérot, J., C, 2016, The Iberian Plate: myth or reality?: Boletin Geologico y Minero, 127, p.
825 557-568.

826 Canérot, J., 2017, The pull apart-type Tardets-Mauléon Basin, a key to understand the
827 formation of the Pyrenees: Bulletin de la Société géologique de France, v. 188, no. 6,
828 p. 35, doi:10.1051/bsgf/2017198.

829 Canérot, J., B. Peybernes, and R. Ciszak, 1978, Présence d'une marge méridionale à
830 l'emplacement de la zone des chainons béarnais (Pyrénées basco-béarnaises): Bulletin
831 de la Société Géologique de France, v. S7-XX, no. 5, p. 673–676,
832 doi:10.2113/gssgfbull.S7-XX.5.673.

833 Canérot, J., and F. Delavaux, 1986, Tectonique et sédimentation sur la marge nord-ibérique
834 des chaînons béarnais (Pyrénées-béarnaises). Remise en question de la signification
835 des lherzolites du sommet de Saraillé: Comptes rendus de l'Académie des sciences.
836 Série 2, v. 302, no. 15, p. 951–956.

837 Canérot, J., and J.-L. Lenoble, 1993, Diapirisme crétacé sur la marge ibérique des Pyrénées
838 occidentales; exemple du pic de Lauriolle; comparaisons avec l'Aquitaine, les
839 Pyrénées centrales et orientales: Bulletin de la Société Géologique de France, v. 164,
840 no. 5, p. 719–726.

841 Canérot, J., C. Majesté-Menjoulas, and Y. Ternet, 1999, Le cadre stratigraphique et
842 géodynamique des altérites et des bauxites sur la marge ibérique des Pyrénées
843 occidentales (France): Comptes Rendus de l'Académie des Sciences-Series II. Earth
844 and Planetary Science, v. 328, no. 7, p. 451–456.

845 Canérot, J., C. Majesté-Menjoulas, and Y. Ternet, 2004, Nouvelle interprétation structurale de
846 la « faille Nord- Pyrénéenne » en vallée d'Aspe (Pyrénées-Atlantiques). Remise en
847 question d'un plutonisme ophitique danien dans le secteur de Bedous: Comptes
848 Rendus Geoscience, v. 336, no. 2, p. 135–142, doi:10.1016/j.crte.2003.11.004.

849 Canérot, J., M. R. Hudec, and K. Rockenbauch, 2005, Mesozoic diapirism in the Pyrenean
850 orogen: Salt tectonics on a transform plate boundary: AAPG Bulletin, v. 89, no. 2, p.
851 211–229, doi:10.1306/09170404007.

852 Casas, A., P. Kearey, L. Rivero, and C. R. Adam, 1997, Gravity anomaly map of the Pyrenean
853 region and a comparison of the deep geological structure of the western and eastern
854 Pyrenees: Earth and Planetary Science Letters, v. 150, no. 1–2, p. 65–78.

855 Casteras, M., 1943, Sur la structure de la partie orientale des Pyrénées basques: Comptes
856 rendus de l'Académie des sciences, v. 216, p. 572–574.

857 Casteras, M., M. Frey, and J. Galharague, 1967, Sur les terrains paléozoïques et sur la
858 structure du massif de Mendibelza (Basses-Pyrénées): Comptes Rendus de l'Académie
859 des Sciences-Série D, v. 264, no. 13, p. 1677–1682.

860 Casteras, M., M. Gottis, M. Clin, J. Guignard, J. Paris, and J. Galharague, 1971, Carte
861 géologique de la France au 1/ 50 000, feuille de Tardets–Sorholus, Orléans, France.

862 Casteras, M., and P. Souquet, 1964, Sur la constitution et sur la structure de la couverture
863 crétacée de la zone primaire axiale pyrénéenne à l'ouest du Pic d'Anie: Comptes
864 rendus de l'Académie des sciences, v. 259, p. 2881–2886.

865 Casteras, M., P. Souquet, G. Culot, and J. Galharague, 1970, Carte géologique de la France au
866 1/50 000: feuille de Larrau, Orléans, France.

867 Chelalou, R., T. Nalpas, R. Bousquet, M. Prevost, A. Lahfid, J. C. Ringenbach, and J. F.
868 Ballard, 2016, New sedimentological, structural and paleo-thermicity data on the

869 Boucheville basin (eastern north Pyrenean zone, France): Compte Rendu Géoscience,
870 doi:10.1016/j.crte.2015.11.008

871 Choukroune, P., 1976, Strain patterns in the Pyrenean chain: Philosophical Transactions of
872 the Royal Society of London A: Mathematical, Physical and Engineering Sciences, v.
873 283, no. 1312, p. 271–280.

874 Choukroune, P., and ECORS Team, 1989, The ECORS Pyrenean deep seismic profile
875 reflection data and the overall structure of an orogenic belt: Tectonics, v. 8, no. 1, p.
876 23–39.

877 Choukroune, P., F. Roure, B. Pinet, and E. P. Team, 1990, Main results of the ECORS
878 Pyrenees profile: Tectonophysics, v. 173, no. 1–4, p. 411–423.

879 Claude, D., 1990, Etude stratigraphique, sédimentologique et structurale des dépôts
880 mésozoïques au nord du massif du Labourd: rôle de la faille de Pamplona (Pays
881 Basque): Université de Bordeaux III, 437 p.

882 Clerc, C., and Y. Lagabrielle, 2014, Thermal control on the modes of crustal thinning leading
883 to mantle exhumation: Insights from the Cretaceous Pyrenean hot paleomargins:
884 Tectonics, v. 33, no. 7, p. 1340–1359, doi:10.1002/2013TC003471.

885 Clerc, C., A. Lahfid, P. Monié, Y. Lagabrielle, C. Chopin, M. Poujol, P. Boulvais, J. C.
886 Ringenbach, E. Masini, and M. de St Blanquat, 2015, High-temperature
887 metamorphism during extreme thinning of the continental crust: a reappraisal of the
888 North Pyrenean passive paleomargin: Solid Earth, v. 6, no. 2, p. 643–668.

889 Combes, P.-J., B. Peybernès, and A. F. Leyreloup, 1998, Altérites et bauxites, témoins des
890 marges européenne et ibérique des Pyrénées occidentales au Jurassique supérieur—
891 Crétacé inférieur, à l'ouest de la vallée d'Ossau (Pyrénées-Atlantiques, France):
892 Comptes Rendus de l'Académie des Sciences-Series II, Earth and Planetary Science,
893 v. 327, no. 4, p. 271–278.

894 Corre, B., Y. Lagabrielle, P. Labaume, S. Fourcade, C. Clerc, and M. Ballèvre, 2016,
895 Deformation associated with mantle exhumation in a distal, hot passive margin
896 environment: New constraints from the Saraillé Massif (Chaînons Béarnais, North-

Pyrenean Zone): Comptes Rendus Geoscience, v. 348, no. 3–4, p. 279–289, doi:10.1016/j.crte.2015.11.007.

Corre, B., 2017, La bordure nord de la plaque ibérique à l'Albo-Cénomanien. Architecture d'une marge passive de type ductile (Chaînons Béarnais, Pyrénées Occidentales): Université de Rennes 1, 320p.

Curnelle, R., 1983, Evolution structuro-sédimentaire du Trias et de l'Infra-Lias d'Aquitaine: Bull. Cent. Rech. Explor. Prod. Elf-Aquitaine, v. 7, no. 1, p. 69–99.

Daignières, M., M. Séguret, M. Specht, and E. Team, 1994, The Arzacq-western Pyrenees ECORS deep seismic profile, *in* Hydrocarbon and petroleum geology of France: Springer, p. 199–208.

Davis, G. H., 1983, Shear-zone model for the origin of metamorphic core complexes: Geology, v. 11, no. 6, p. 342–347, doi:10.1130/0091-7613(1983)11<342:SMFTOO>2.0.CO;2.

Davis, G. A., G. S. Lister, and S. J. Reynolds, 1986, Structural evolution of the Whipple and South mountains shear zones, southwestern United States: Geology, v. 14, no. 1, p. 7–10, doi:10.1130/0091-7613(1986)14<7:SEOTWA>2.0.CO;2.

Debroas, E. J., J. Canérot, and M. Bilotte, 2010, Les brèches d'Urdach, témoins de l'exhumation du manteau pyrénéen dans un escarpement de faille vraconnien-cénomanien inférieur (Zone nord-pyrénéenne, Pyrénées-Atlantiques, France): Géologie de la France, v. 2, p. 53–63.

Decarlis, A., G. Manatschal, I. Haupert, and E. Masini, 2015, The tectono-stratigraphic evolution of distal, hyper-extended magma-poor conjugate rifted margins: Examples from the Alpine Tethys and Newfoundland–Iberia: Marine and Petroleum Geology, v. 68, p. 54–72, doi:10.1016/j.marpetgeo.2015.08.005.

Delfaud, J., and J. Henry, 1967, Evolution des bassins jurassiques dans la zone nord-pyrénéenne occidentale: 64ème congrès AFAS Bordeaux, p. 75–80.

Delfaud, J., and M. Villanova, 1967, Evolution des bassins pendant le Crétacé inférieur dans les Pyrénees occidentales et la bordure de l'Aquitaine: 64ème congrès AFAS Bordeaux, p. 87–92.

Díaz, J., D. Pedreira, M. Ruiz, J. A. Pulgar, and J. Gallart, 2012, Mapping the indentation between the Iberian and Eurasian plates beneath the Western Pyrenees/Eastern Cantabrian Mountains from receiver function analysis: Tectonophysics, v. 570–571, p. 114–122, doi:10.1016/j.tecto.2012.07.005.

Ducasse, L., and P.-C. Vélasque, 1988, Géotraverse dans la partie occidentale des Pyrénées, de l'avant-pays aquitain au bassin de l'Ebre: effet d'une inversion structurale sur l'édification d'une chaîne intracontinentale: Université Paul Cézanne (Aix-Marseille). Faculté des sciences et techniques de Saint-Jérôme, 287 p.

Ducasse, L., P.-C. Vélasque, and J. Muller, 1986, Glissement de couverture et panneaux basculés dans la région des Arbailles (Pyrénées occidentales): Un modèle évolutif crétacé de la marge nord-ibérique à l'Est de la transformante de Pamplona: Comptes rendus de l'Académie des sciences. Série 2, Mécanique, Physique, Chimie, Sciences de l'univers, Sciences de la Terre, v. 303, no. 16, p. 1477–1482.

Ducoux, M., 2017, Structure, thermicité et évolution géodynamique de la Zone Interne Métamorphique des Pyrénées. PhD thesis, University of Orléans, France, 646 p.

Duée, G., Y. Lagabrielle, A. Coutelle, and A. Fortané, 1984, Les lherzolites associées aux Chaînons Béarnais (Pyrénées Occidentales): Mise à l'affleurement anté-dogger et resédimentation albo-cénomanienne: Comptes-rendus des séances de l'Académie des sciences. Série 2, Mécanique-physique, chimie, sciences de l'univers, sciences de la terre, v. 299, no. 17, p. 1205–1210.

Dumont, T., Replumaz, A., Rouméjon, S., Briais, A., Rigo, A., Bouillin, J.-P., 2015. Microseismicity of the Béarn range: Reactivation of inversion and collision structures at the northern edge of the Iberian plate: SEISMICITY AND STRUCTURES IN W. PYRENEES. Tectonics 34, 934–950. https://doi.org/10.1002/2014TC003816

Durand-Wackenheim, C., P. Souquet, and G. Thiébaut, 1981, La brèche d'Errozaté (Pyrénées-Atlantiques): faciès de résedimentation en milieu profond de matériaux d'une

952 plateforme carbonatée crétacée à substratum hercynien: Bulletin de la Société
953 d'Histoire Naturelle de Toulouse, v. 117, p. 87–94.

954 Engeser, T., and W. Schwentke, 1986, Towards a new concept of the tectogenesis of the
955 Pyrenees: Tectonophysics, v. 129, no. 1–4, p. 233–242, doi:10.1016/0040-
956 1951(86)90253-2.

957 Etheve, N., 2016, Le bassin de Valence à la frontière des domaines ibérique et méditerranéen:
958 Evolution tectonique et sédimentaire du Mésozoïque au Cénozoïque: Université de
959 Cergy Pontoise, 291 p.

960 Etheve, N., G. Mohn, D. Frizon de Lamotte, E. Roca, J. Tugend and J. Gomez-Romeu, 2018,
961 Extreme Mesozoic Crustal Thinning in the Eastern Iberia Margin: The Example of the
962 Columbrets Basin (Valencia Trough): Tectonics, n° 37, doi: 10.1002/2017TC004613.

963 Fabriès, J., J.-P. Lorand, and J.-L. Bodinier, 1998, Petrogenetic evolution of orogenic
964 lherzolite massifs in the central and western Pyrenees: Tectonophysics, v. 292, no. 1–
965 2, p. 145–167.

966 Fabriès, J., J.-P. Lorand, J.-L. Bodinier, and C. Dupuy, 1991, Evolution of the Upper Mantle
967 beneath the Pyrenees: Evidence from Orogenic Spinel Lherzolite Massifs: Journal of
968 Petrology, v. Special_Volume, no. 2, p. 55–76,
969 doi:10.1093/petrology/Special_Volume.2.55.

970 Ferrer, O., M. P. A. Jackson, E. Roca, and M. Rubinat, 2012, Evolution of salt structures
971 during extension and inversion of the Offshore Parentis Basin (Eastern Bay of
972 Biscay): Geological Society, London, Special Publications, v. 363, no. 1, p. 361–380,
973 doi:10.1144/SP363.16.

974 Ferrer, O., E. Roca, B. Benjumea, J. A. Muñoz, N. Ellouz, and MARCONI Team, 2008, The
975 deep seismic reflection MARCONI-3 profile: Role of extensional Mesozoic structure
976 during the Pyrenean contractional deformation at the eastern part of the Bay of Biscay:
977 Marine and Petroleum Geology, v. 25, no. 8, p. 714–730,
978 doi:10.1016/j.marpetgeo.2008.06.002.

979 Fixari, G., 1984, Stratigraphie, faciès et dynamique tecto-sédimentaire du flysch albien
980 (flysch noir et poudingues de mendibelza) dans la région de Mauléon-Tardets
981 (Pyrénées Atlantiques): Université Paul Sabatier de Toulouse (Sciences), 197 p.

982 Fortané, A., G. Duée, Y. Lagabrielle, and A. Coutelle, 1986, Lherzolites and the western
983 "Chaînons Béarnais" (French Pyrenees): Structural and paleogeographical pattern:
984 Tectonophysics, v. 129, no. 1–4, p. 81–98, doi:10.1016/0040-1951(86)90247-7.

985 Fournier, E., 1905, Études géologiques sur la partie occidentale de la chaîne des Pyrénées
986 entre la vallée d'Aspe et celle de la Nive: Bulletin de la Société Géologique de France,
987 v. 5, p. 699–723.

988 Fournier, E., 1908, Etudes sur les Pyrénées Basques:(Basses-Pyrénées, Navarre et
989 Guipuzcoa): Bulletin des services de la carte géologique de la France et des
990 topographies souterraines, v. 18, no. 121, p. 491–548.

991 Galharague, J., 1966, Étude géologique de la zone de relais des massifs d'Igounce et de
992 Mendibelza (Basses-Pyrénées).

993 Geoffroy, L., B. Le Gall, M. A. Daoud, and M. Jalludin, 2014, Flip-flop detachment tectonics
994 at nascent passive margins in SE Afar: Journal of the Geological Society, v. 171, no.
995 5, p. 689–694, doi:10.1144/jgs2013-135.

996 Gillard, M., J. Autin, G. Manatschal, D. Sauter, M. Munschy, and M. Schaming, 2015,
997 Tectonomagmatic evolution of the final stages of rifting along the deep conjugate
998 Australian-Antarctic magma-poor rifted margins: Constraints from seismic
999 observations: Australian-Antarctic margins evolution: Tectonics, v. 34, no. 4, p. 753–
1000 783, doi:10.1002/2015TC003850.

1001 Golberg, J. M., and A. F. Leyreloup, 1990, High temperature-low pressure Cretaceous
1002 metamorphism related to crustal thinning (Eastern North Pyrenean Zone, France):
1003 Contributions to Mineralogy and Petrology, v. 104, no. 2, p. 194–207,
1004 doi:10.1007/BF00306443.

1005 Golberg, J.-M., and H. Maluski, 1988, Données nouvelles et mise au point sur l'âge du
1006 métamorphisme pyrénéen: Comptes rendus de l'Académie des sciences. Série 2, v.
1007 306, no. 6, p. 429–435.

1008 Gong, Z., C. G. Langereis, and T. A. T. Mullender, 2008, The rotation of Iberia during the
1009 Aptian and the opening of the Bay of Biscay: Earth and Planetary Science Letters, v.
1010 273, no. 1–2, p. 80–93, doi:10.1016/j.epsl.2008.06.016.

1011 Grandjean, G., 1992, Mise en évidence des structures crustales dans une portion de chaîne et
1012 de leur relation avec les bassins sédimentaires. Application aux Pyrénées occidentales
1013 au travers du Projet ECORS Arzacq-Pyrénées: Université des Sciences et Techniques
1014 du Languedoc, 291 p.

1015 Grandjean, G., 1994, Etude des structures crustales dans une portion de chaîne et de leur
1016 relation avec les bassins sédimentaires. Application aux Pyrénées occidentales: Bull.
1017 Cent. Rech. Explor. Prod. Elf Aquitaine, v. 18, no. 2, p. 391–420.

1018 Gubler, Y., M. Casteras, R. Ciry, and P. Lamare, 1947, Sur l'âge des poudingues dits de
1019 Mendibelza dans le bassin du Laurhibar, au SE de Mendive (Basse Pyrénées: Compte
1020 Rendu de la Société Géologique de France, v. 17, p. 329–330.

1021 Hall, C. A., and J. A. Johnson, 1986, Apparent western termination of the North Pyrenean
1022 fault and tectonostratigraphic units of the western north Pyrenees, France and Spain:
1023 Tectonics, v. 5, no. 4, p. 607–627.

1024 Hart, N. R., D. F. Stockli, and N. W. Hayman, 2016, Provenance evolution during progressive
1025 rifting and hyperextension using bedrock and detrital zircon U-Pb geochronology,
1026 Mauléon Basin, western Pyrenees: Geosphere, v. 12, no. 4, p. 1166–1186,
1027 doi:10.1130/GES01273.1.

1028 Hart, N. R., D. F. Stockli, L. L. Lavier, and N. W. Hayman, 2017, Thermal evolution of a
1029 hyperextended rift basin, Mauléon Basin, western Pyrenees: Thermal evolution of
1030 hyperextended rift: Tectonics, doi:10.1002/2016TC004365.

1031 Haupert, I., G. Manatschal, A. Decarlis, and P. Unternehr, 2016, Upper-plate magma-poor
1032 rifted margins: Stratigraphic architecture and structural evolution: Marine and
1033 Petroleum Geology, v. 69, p. 241–261, doi:10.1016/j.marpetgeo.2015.10.020.

1034 Heddebaut, C., 1973, Etudes géologiques dans les massifs paléozoïques basques: Université
1035 des Sciences et Techniques de Lille, 263 p.

1036 Heddebaut, C., 1967, Observations tectoniques sur le massif des Aldudes (Basses-Pyrénées):
1037 CR Som. Soc. Géol. de France, fasc, v. 7, p. 280–281.

1038 Henry, J., G. Zolnaï, G. Le Pochat, and C. Mondeilh, 1987, Carte géologique de la France au
1039 1/50 000: feuille d'Orthez, Orléans, France.

1040 Huismans, R. S., and C. Beaumont, 2003, Symmetric and asymmetric lithospheric extension:
1041 Relative effects of frictional-plastic and viscous strain softening: Journal of
1042 Geophysical Research: Solid Earth, v. 108, no. B10, doi:10.1029/2002JB002026.

1043 Huismans, R. S., and C. Beaumont, 2008, Complex rifted continental margins explained by
1044 dynamical models of depth-dependent lithospheric extension: Geology, v. 36, no. 2, p.
1045 163, doi:10.1130/G24231A.1.

1046 Huismans, R. S., and C. Beaumont, 2011, Depth-dependent extension, two-stage breakup and
1047 cratonic underplating at rifted margins: Nature, v. 473, no. 7345, p. 74–78,
1048 doi:10.1038/nature09988.

1049 Huismans, R. S., and C. Beaumont, 2014, Rifted continental margins: The case for depth-
1050 dependent extension: Earth and Planetary Science Letters, v. 407, p. 148–162,
1051 doi:10.1016/j.epsl.2014.09.032.

1052 James, V., 1998, La plate-forme carbonatée ouest-pyrénéenne au jurassique moyen et
1053 supérieur stratigraphie séquentielle, stades d'évolution, relations avec la subsurface en
1054 aquitaine méridionale: Toulouse, Université Paul Sabatier (Sciences), 351 p.

1055 James, V., and J. Canérot, 1999, Diapirisme et structuration post-triasique des Pyrénées
1056 occidentales et de l'Aquitaine méridionale (France): Eclogae Geologicae Helvetiae, v.
1057 92, p. 63–72.

1058 Jammes, S., G. Manatschal, L. Lavier, and E. Masini, 2009, Tectono-sedimentary evolution
1059 related to extreme crustal thinning ahead of a propagating ocean: Example of the
1060 western Pyrenees: Tectonics, v. 28, no. 4, doi:10.1029/2008TC002406.

1061 Jammes, S., G. Manatschal, and L. Lavier, 2010a, Interaction between prerift salt and
1062 detachment faulting in hyperextended rift systems: The example of the Parentis and

1063 Mauléon basins (Bay of Biscay and western Pyrenees): AAPG Bulletin, v. 94, no. 7, p.
1064 957–975, doi:10.1306/12090909116.

1065 Jammes, S., C. Tiberi, and G. Manatschal, 2010b, 3D architecture of a complex transcurrent
1066 rift system: The example of the Bay of Biscay–Western Pyrenees: Tectonophysics, v.
1067 489, no. 1–4, p. 210–226, doi:10.1016/j.tecto.2010.04.023.

1068 Johnson, J. A., and C. A. Hall, 1989, Tectono-stratigraphic model for the Massif D'Igountze-
1069 Mendibelza, western Pyrenees: Journal of the Geological Society, v. 146, no. 6, p.
1070 925–932, doi:10.1144/gsjgs.146.6.0925.

1071 Karner, G. D., N. W. Driscoll, and D. H. N. Barker, 2003, Syn-rift regional subsidence across
1072 the West African continental margin: the role of lower plate ductile extension:
1073 Geological Society, London, Special Publications, v. 207, no. 1, p. 105–129,
1074 doi:10.1144/GSL.SP.2003.207.6.

1075 Labaume, P., F. Meresse, M. Jolivet, and A. Teixell, 2016, Exhumation sequence of the
1076 basement thrust units in the west-central Pyrenees. Constraints from apatite fission
1077 track analysis: Geogaceta, v. 60, p. 11–14.

1078 Lagabrielle, Y., and J.-L. Bodinier, 2008, Submarine reworking of exhumed sub-continental
1079 mantle rocks: field evidence from the Lherz peridotites, French Pyrenees: Cretaceous
1080 exhumation of pyrenean mantle: Terra Nova, v. 20, no. 1, p. 11–21,
1081 doi:10.1111/j.1365-3121.2007.00781.x.

1082 Lagabrielle, Y., C. Clerc, A. Vauchez, A. Lahfid, P. Labaume, B. Azambre, S. Fourcade, and
1083 J.-M. Dautria, 2016, Very high geothermal gradient during mantle exhumation
1084 recorded in mylonitic marbles and carbonate breccias from a Mesozoic Pyrenean
1085 palaeomargin (Lherz area, North Pyrenean Zone, France): Comptes Rendus
1086 Geoscience, v. 348, no. 3–4, p. 290–300, doi:10.1016/j.crte.2015.11.004.

1087 Lagabrielle, Y., P. Labaume, and M. de Saint Blanquat, 2010, Mantle exhumation, crustal
1088 denudation, and gravity tectonics during Cretaceous rifting in the Pyrenean realm (SW
1089 Europe): Insights from the geological setting of the lherzolite bodies: Tectonics, v. 29,
1090 no. 4, doi:10.1029/2009TC002588.

1091 Lamare, P., 1939, La série paléozoïque du massif du Baygoura et de la vallée de la Nive; ses
1092 relations avec les terrains secondaires environnants: Bulletin de la Société Géologique
1093 de France, v. 9, p. 163–184.

1094 Lamare, P., 1944, La terminaison orientale du massif des Aldudes, aux environs d'Arnéguy,
1095 révision de la feuille de Saint-Jean-Pied-de-Port au 1/80 000: Bulletin de la Carte
1096 Géologique de France, v. 45, no. 216, p. 265–305.

1097 Lamare, P., 1946, Les formations détritiques crétacées du massif de Mendibelza: Bulletin de
1098 la Socèté Géologique de France, v. 16, no. 5, p. 265–312.

1099 Lamare, P., 1941, Remarques sur la structure du Pays Basques: Bulletin de la Societe
1100 Geologique de France, v. 11, p. 97–112.

1101 Lamare, P., 1948, Sur le passage latéral des faciès détritiques grossiers du Crétacé du massif
1102 de Mendibelza aux faciès schisto-gréseux classiques de l'Albien des Pyrénées:
1103 Comptes rendus de l'Académie des sciences, v. 226, no. 8, p. 683–685.

1104 Larrasoaña, J. C., J. M. Parés, H. Millán, J. del Valle, and E. L. Pueyo, 2003, Paleomagnetic,
1105 structural, and stratigraphic constraints on transverse fault kinematics during basin
1106 inversion: The Pamplona Fault (Pyrenees, north Spain): Tectonics, v. 22, no. 6,
1107 doi:10.1029/2002TC001446.

1108 Laverdière, J.-W., 1930, Les formations paléozoïques de la vallée du Laurhibar: Mém. Soc.
1109 Géol. Nord. Lille, v. 55, p. 156–157.

1110 Lavier, L. L., and G. Manatschal, 2006, A mechanism to thin the continental lithosphere at
1111 magma-poor margins: Nature, v. 440, no. 7082, p. 324–328, doi:10.1038/nature04608.

1112 Le Pichon, X., J. Bonnin, U. J. Francheteau and J. C. Sibuet, 1971, Une hypothèse d'évolution
1113 tectonique du golfe de Gascogne. In : Histoire structurale du golfe de Gascogne, ed
1114 Technip., IV, 11, p. 1-44.

1115 Le Pochat, G., C. Bolthenhagen, M. Lenguin, S. Lorsignol, and C. Thibault, 1976, Carte
1116 géologique de France au 1/50 000: Mauléon-licharre, Orléans, France.

1117 Le Pochat, G., C. Heddebaut, M. Lenguin, S. Lorsignol, P. Souquet, J. Muller, and P. Roger,
1118 1978, Carte Géologique de France au 1/50 000: St Jean Pied de Port, Orléans, France.

1119 Lenoble, J.-L., 1992, Les plates-formes carbonatées ouest-pyrénéennes du dogger à l'Albien,
1120 stratigraphie séquentielle et évolution géodynamique: Université Paul Sabatier de
1121 Toulouse (Sciences), 395 p.

1122 Lister, G. S., M. A. Etheridge, and P. A. Symonds, 1986, Detachment faulting and the
1123 evolution of passive continental margins: Geology, v. 14, no. 3, p. 246–250,
1124 doi:10.1130/0091-7613(1986)14<246:DFATEO>2.0.CO;2.

1125 Lucas, C., 1985, Le grès rouge du versant nord des Pyrénées: essai sur la géodynamique de
1126 dépôts continentaux du permien et du trias: 267 p.

1127 Magné, 1948, Nouvelles observations relatives à l'âge des poudingues du pic Errozaté (massif
1128 de Mendibelza): Compte Rendu de la Société Géologique de France, p. 163–165.

1129 Malod, J., A, 1982, Comparaison de l'évolution des marges continentales au nord et au sud de
1130 la péninsule ibérique. PhD thesis ('Thèse d'état'), University of Paris, France, 235 p.

1131 Manatschal, G., 2004, New models for evolution of magma-poor rifted margins based on a
1132 review of data and concepts from West Iberia and the Alps: International Journal of
1133 Earth Sciences, v. 93, no. 3, doi:10.1007/s00531-004-0394-7.

1134 Manatschal, G., A. Engström, L. Desmurs, U. Schaltegger, M. Cosca, O. Müntener, and D.
1135 Bernoulli, 2006, What is the tectono-metamorphic evolution of continental break-up:
1136 The example of the Tasna Ocean–Continent Transition: Journal of Structural Geology,
1137 v. 28, no. 10, p. 1849–1869, doi:10.1016/j.jsg.2006.07.014.

1138 Masini, E., G. Manatschal, G. Mohn, J.-F. Ghienne, and F. Lafont, 2011, The tectono-
1139 sedimentary evolution of a supra-detachment rift basin at a deep-water magma-poor
1140 rifted margin: the example of the Samedan Basin preserved in the Err nappe in SE
1141 Switzerland: Tectono-sedimentary evolution of a supra-detachment rift basin: Basin
1142 Research, v. 23, no. 6, p. 652–677, doi:10.1111/j.1365-2117.2011.00509.x.

1143 Masini, E., G. Manatschal, G. Mohn, and P. Unternehr, 2012, Anatomy and tectono-
1144 sedimentary evolution of a rift-related detachment system: The example of the Err
1145 detachment (central Alps, SE Switzerland): Geological Society of America Bulletin, v.
1146 124, no. 9–10, p. 1535–1551, doi:10.1130/B30557.1.

1147 Masini, E., G. Manatschal, and G. Mohn, 2013, The Alpine Tethys rifted margins:
1148 Reconciling old and new ideas to understand the stratigraphic architecture of magma-
1149 poor rifted margins: Sedimentology, v. 60, no. 1, p. 174–196, doi:10.1111/sed.12017.

1150 Masini, E., G. Manatschal, J. Tugend, G. Mohn, and J.-M. Flament, 2014, The tectono-
1151 sedimentary evolution of a hyper-extended rift basin: the example of the Arzacq–
1152 Mauléon rift system (Western Pyrenees, SW France): International Journal of Earth
1153 Sciences, v. 103, no. 6, p. 1569–1596, doi:10.1007/s00531-014-1023-8.

1154 Mattauer, M., 1985, Présentation d'un modèle lithosphérique de la chaîne des Pyrénées:
1155 Comptes-rendus des séances de l'Académie des sciences. Série 2, Mécanique-
1156 physique, chimie, sciences de l'univers, sciences de la terre, v. 300, no. 2, p. 71–74.

1157 McCaig, A. M., 1988, Deep geology of the Pyrenees: Nature, v. 331, p. 480–481.

1158 McKenzie, D., 1978, Some remarks on the development of sedimentary basins: Earth and
1159 Planetary Science Letters, v. 40, no. 1, p. 25–32, doi:10.1016/0012-821X(78)90071-7.

1160 Merle, J.-M., 1974, Recherches sur les relations paléogéographiques et structurales entre les
1161 massifs basques au sud de Saint-Jean-Pied-de-Port (Pyrénées occidentales): Université
1162 Paul Sabatier de Toulouse (Sciences), 142 p.

1163 Mirouse, R., 1967, Le Dévonien des Pyrénées occidentales et centrales (France): International
1164 Symposium on the Devonian System, v. I, p. 153–170.

1165 Mohn, G., Manatschal, G., Beltrando, and M., Haupert, I., 2014, The role of rift-inherited
1166 hyper-extension in Alpine-type orogens: Terra Nova, v. 26, p. 347–353, doi:
1167 10.1111/ter.12104.

1168 Montigny, R., B. Azambre, M. Rossy, and R. Thuizat, 1986, K-Ar Study of cretaceous
1169 magmatism and metamorphism in the Pyrenees: Age and length of rotation of the
1170 Iberian Peninsula: Tectonophysics, v. 129, no. 1, p. 257–273, doi:10.1016/0040-
1171 1951(86)90255-6.

1172 Mouthereau, F., P.-Y. Filleaudeau, A. Vacherat, R. Pik, O. Lacombe, M. G. Fellin, S.
1173 Castelltort, F. Christophoul, and E. Masini, 2014, Placing limits to shortening
1174 evolution in the Pyrenees: Role of margin architecture and implications for the

1175 Iberia/Europe convergence: Tectonics, v. 33, no. 12, p. 2014TC003663,
1176 doi:10.1002/2014TC003663.

1177 Muller, J., and P. Roger, 1977, L'Evolution structurale des Pyrénées (Domaine central et
1178 occidental) Le segment hercynien, la chaîne de fond alpine: Géologie alpine, v. 53, no.
1179 2, p. 149–191.

1180 Muñoz, J. A., 1992, Evolution of a continental collision belt: ECORS-Pyrenees crustal
1181 balanced cross-section, *in* K. R. McClay, ed., Thrust Tectonics: Springer Netherlands,
1182 p. 235–246, doi:10.1007/978-94-011-3066-0_21.

1183 Olivet, J. L., 1996, La cinématique de la plaque ibérique: Bull. Cent. Rech. Explor. Prod. Elf
1184 Aquitaine, v. 20, no. 1, p. 131–195.

1185 Paris, J.-P., 1964, Étude d'une partie du massif d'Igounce et de ses abords septentrionaux en
1186 Barétous et Basse-Soule: Faculté des Sciences de l'Université de Toulouse, 121 p.

1187 Pedreira, D., J. A. Pulgar, J. Gallart, and M. Torné, 2007, Three-dimensional gravity and
1188 magnetic modeling of crustal indentation and wedging in the western Pyrenees-
1189 Cantabrian Mountains: Journal of Geophysical Research, v. 112, no. B12,
1190 doi:10.1029/2007JB005021.

1191 Péron-Pinvidic, G., G. Manatschal, T. A. Minshull, and D. S. Sawyer, 2007, Tectono-
1192 sedimentary evolution of the deep Iberia-Newfoundland margins: Evidence for a
1193 complex breakup history: Tectonics, v. 26, no. 2, p. 1–19,
1194 doi:10.1029/2006TC001970.

1195 Péron-Pinvidic, G., G. Manatschal, E. Masini, E. Sutra, J. M. Flament, I. Haupert, and P.
1196 Unternehr, 2015, Unravelling the along-strike variability of the Angola–Gabon rifted
1197 margin: a mapping approach: Geological Society, London, Special Publications, v.
1198 438, no. 1, p. 49–76, doi:10.1144/SP438.1.

1199 Pinet, B., L. Montadert, and ECORS Scientific Party, 1987, Deep seismic reflection and
1200 refraction profiling along the Aquitaine shelf (Bay of Biscay): Geophysical Journal
1201 International, v. 89, no. 1, p. 305–312, doi:10.1111/j.1365-246X.1987.tb04423.x.

1202 Poignant, A., 1965, Révision du Crétacé inférieur en Aquitaine occidentale et méridionale:
1203 Université Paris, 317 p.

1204 Puigdefàbregas, C., and P. Souquet, 1986, Tecto-sedimentary cycles and depositional
1205 sequences of the Mesozoic and Tertiary from the Pyrenees: Tectonophysics, v. 129,
1206 no. 1–4, p. 173–203.

1207 Rat, P. et al., 1983, Vue sur le Cretacé basco-cantabrique et nord-ibérique: Une marge et son
1208 arriere-pays, ses environnements sedimentaires: Memoires geologiques Universite de
1209 Dijon, v. 9, p. 191.

1210 Ravier, J., 1957, Le métamorphisme des terrains secondaires des Pyrénées: Université,
1211 Faculté des Sciences.

1212 Razin, P., 1989, Evolution tecto-sédimentaire alpine des Pyrénées basques à l'ouest de la
1213 transformante de Pamplona, Province du Labourd: Université Bordeaux 3, 464 p.

1214 Richard, P., 1986, Structure et évolution alpine des massifs paléozoïques du Labourd (Pays
1215 Basque français): Éditions du Bureau de recherches géologiques et minières, 374 p.

1216 Roca, E., J. A. Muñoz, O. Ferrer, and N. Ellouz, 2011, The role of the Bay of Biscay
1217 Mesozoic extensional structure in the configuration of the Pyrenean orogen:
1218 Constraints from the MARCONI deep seismic reflection survey: Tectonics, v. 30, no.
1219 2, doi:10.1029/2010TC002735.

1220 Roest, W. R and S. P. Srivastava., 1991, Kinematics of the plate boundaries between Eurasia,
1221 Iberia ,and Africa in the North Atlantic from the Late Cretaceous to the present:
1222 Geology, v. 19, p. 613–616.

1223 Rosenbaum, G., G. S. Lister, and C. Duboz, 2002, Relative motions of Africa, Iberia and
1224 Europe during Alpine orogeny: Tectonophysics, v. 359, no. 1–2, p. 117–129,
1225 doi:10.1016/S0040-1951(02)00442-0.

1226 Rossi, P., A. Cocherie, C. M. Fanning, and Y. Ternet, 2003, Datation U-Pb sur zircons des
1227 dolérites tholéiitiques pyrénéennes (ophites) à la limite Trias–Jurassique et relations
1228 avec les tufs volcaniques dits « infra-liasiques » nord-pyrénéens: Comptes Rendus
1229 Geoscience, v. 335, no. 15, p. 1071–1080, doi:10.1016/j.crte.2003.09.011.

1230 Roux, J.-C., 1983, Recherches stratigraphiques et sédimentologiques sur les flyschs crétacés
1231 pyrénéens au sud d'Oloron (Pyrénées Atlantiques): Université Paul Sabatier de
1232 Toulouse (Sciences), 224 p.

1233 Sauter, D., M. Cannat, S. Rouméjon, M. Andreani, D. Birot, A. Bronner, D. Brunelli, J.
1234 Carlut, A. Delacour, and V. Guyader, 2013, Continuous exhumation of mantle-derived
1235 rocks at the Southwest Indian Ridge for 11 million years: Nature Geoscience, v. 6, no.
1236 4, p. 314.

1237 Séguret, M., and M. Daignières, 1986, Crustal scale balanced cross-sections of the Pyrenees;
1238 discussion: Tectonophysics, v. 129, no. 1, p. 303–318, doi:10.1016/0040-
1239 1951(86)90258-1.

1240 Serrano, O., J. Delmas, F. Hanot, R. Vially, J.-P. Herbin, P. Houel, and B. Tourlière, 2006, Le
1241 bassin d'Aquitaine: valorisation des données sismiques, cartographie structurale et
1242 potentiel pétrolier: Bureau de Recherche Géologique et minière, 245 p.

1243 Sibuet, J.-C., S. P. Srivastava, and W. Spakman, 2004, Pyrenean orogeny and plate
1244 kinematics: Journal of Geophysical Research: Solid Earth, v. 109, no. B8, p. B08104,
1245 doi:10.1029/2003JB002514.

1246 Souquet, P., 1988, Evolución del margen noribérico en los Pyreneos durante el Mesozoico:
1247 Rev. Soc. Geol. España, v. 1, p. 349–356.

1248 Souquet, P., 1967, Le Crétacé supérieur Sud-Pyrénéen, en Catalogne, Aragon et Navarre: E.
1249 Privat.

1250 Souquet, P., B. Peybernes, M. Bilotte, and E.-J. Debroas, 1977, La chaîne alpine des
1251 Pyrénées: Géologie alpine, v. 53, no. 2, p. 193–216.

1252 Souquet, P. et al., 1985, Le groupe du Flysch noir (albo-cénomanien) dans les Pyrénées: Bull
1253 Cent. Rech Exlpo-Prod Elf-Aquitaine Pau, v. 9, p. 183–252.

1254 Spencer, J. E., 1984, Role of tectonic denudation in warping and uplift of low-angle normal
1255 faults: Geology, v. 12, no. 2, p. 95–98, doi:10.1130/0091-
1256 7613(1984)12<95:ROTDIW>2.0.CO;2.

1257 Svartman Dias, A. E., L. L. Lavier, and N. W. Hayman, 2015, Conjugate rifted margins width
1258 and asymmetry: The interplay between lithospheric strength and thermomechanical
1259 processes: Journal of Geophysical Research: Solid Earth, v. 120, no. 12, p.
1260 2015JB012074, doi:10.1002/2015JB012074.

1261 Teixell, A., 1993, Coupe géologique du massif d'Igountze: implications sur l'évolution
1262 structurale de la bordure sud de la zone nord-pyrénéenne occidentale: Comptes rendus
1263 de l'Académie des sciences. Série 2, Mécanique, Physique, Chimie, Sciences de
1264 l'univers, Sciences de la Terre, v. 316, no. 12, p. 1789–1796.

1265 Teixell, A., 1996, The Anso transect of the southern Pyrenees: basement and cover thrust
1266 geometries: Journal of the Geological Society, v. 153, no. 2, p. 301–310,
1267 doi:10.1144/gsjgs.153.2.0301.

1268 Teixell, A., 1998, Crustal structure and orogenic material budget in the west central Pyrenees:
1269 Tectonics, v. 17, no. 3, p. 395–406, doi:10.1029/98TC00561.

1270 Teixell, A., P. Labaume, and Y. Lagabrielle, 2016, The crustal evolution of the west-central
1271 Pyrenees revisited: Inferences from a new kinematic scenario: Comptes Rendus
1272 Geoscience, v. 348, no. 3–4, p. 257–267, doi:10.1016/j.crte.2015.10.010.

1273 Tirel, C., J.-P. Brun, and E. Burov, 2004, Thermomechanical modeling of extensional gneiss
1274 domes: Geological Society of America Special Papers, v. 380, p. 67–78,
1275 doi:10.1130/0-8137-2380-9.67.

1276 Tugend, J., G. Manatschal, N. J. Kusznir, E. Masini, G. Mohn, and I. Thinon, 2014,
1277 Formation and deformation of hyperextended rift systems: Insights from rift domain
1278 mapping in the Bay of Biscay-Pyrenees: Tectonics, v. 33, no. 7, p. 1239–1276,
1279 doi:10.1002/2014TC003529.

1280 Tugend, J., G. Manatschal, N. J. Kusznir, and E. Masini, 2015a, Characterizing and
1281 identifying structural domains at rifted continental margins: application to the Bay of
1282 Biscay margins and its Western Pyrenean fossil remnants: Geological Society,
1283 London, Special Publications, v. 413, no. 1, p. 171–203, doi:10.1144/SP413.3.

1284 Tugend, J., G. Manatschal, and N. J. Kusznir, 2015b, Spatial and temporal evolution of
1285 hyperextended rift systems: Implication for the nature, kinematics, and timing of the
1286 Iberian-European plate boundary: Geology, v. 43, p. 15–18, doi: 10.1130/G36072.1.

1287 Unternehr, P., G. Peron-Pinvidic, G. Manatschal, and E. Sutra, 2010, Hyper-extended crust in
1288 the South Atlantic: in search of a model: Petroleum Geoscience, v. 16, no. 3, p. 207–
1289 215, doi:10.1144/1354-079309-904.

1290 Vacherat, A., F. Mouthereau, R. Pik, M. Bernet, C. Gautheron, E. Masini, L. Le Pourhiet, B.
1291 Tibari, and A. Lahfid, 2014, Thermal imprint of rift-related processes in orogens as
1292 recorded in the Pyrenees: Earth Planet. Sci. Lett.,408, 296–306,
1293 doi:10.1016/j.epsl.2014.10.014.

1294 Vergés, J., H. Millán, E. Roca, J. A. Muñoz, M. Marzo, J. Cirés, T. D. Bezemer, R.
1295 Zoetemeijer, and S. Cloetingh, 1995, Eastern Pyrenees and related foreland basins:
1296 pre-, syn- and post-collisional crustal-scale cross-sections: Marine and Petroleum
1297 Geology, v. 12, no. 8, p. 903–915, doi:10.1016/0264-8172(95)98854-X.

1298 Viennot, P., and Y. Kieh, 1928, Observations pétrographiques dans le massif cristallin du
1299 Labourd (Basses Pyrénées): Bull. Soc. Géol. Fr, v. 28, p. 369–379.

1300 Viers, G., 1956, Observations structurales sur les Pyrénées occidentales: Bull. Soc. géol.
1301 France, v. 6, no. 6, p. 713–726.

1302 Wang, Y., 2017, High resolution imaging of lithospheric structures by full waveform
1303 inversion of short period teleseismic P waves: Université Toulouse 3 Paul Sabatier
1304 (UT3 Paul Sabatier), 244 p.

1305 Wang, Y. et al., 2016, The deep roots of the western Pyrenees revealed by full waveform
1306 inversion of teleseismic P waves: Geology, v. 44, no. 6, p. 475–478,
1307 doi:10.1130/G37812.1.

1308 Wernicke, B., 1981, Low-angle normal faults in the Basin and Range Province: nappe
1309 tectonics in an extending orogen: Nature, v. 291, no. 5817, p. 645–648,
1310 doi:10.1038/291645a0.

1311 Wernicke, B., 1985, Uniform-sense normal simple shear of the continental lithosphere:
1312 Canadian Journal of Earth Sciences, v. 22, no. 1, p. 108–125, doi:10.1139/e85-009.

1313 Wernicke, B., and B. C. Burchfiel, 1982, Modes of extensional tectonics: Journal of Structural
1314 Geology, v. 4, no. 2, p. 105–115, doi:10.1016/0191-8141(82)90021-9.

1315 Wernicke, B., and G. J. Axen, 1988, On the role of isostasy in the evolution of normal fault
1316 systems: Geology, v. 16, no. 9, p. 848–851, doi:10.1130/0091-
1317 7613(1988)016<0848:OTROII>2.3.CO;2.

1318

Figures and Captions:

Figure. 1

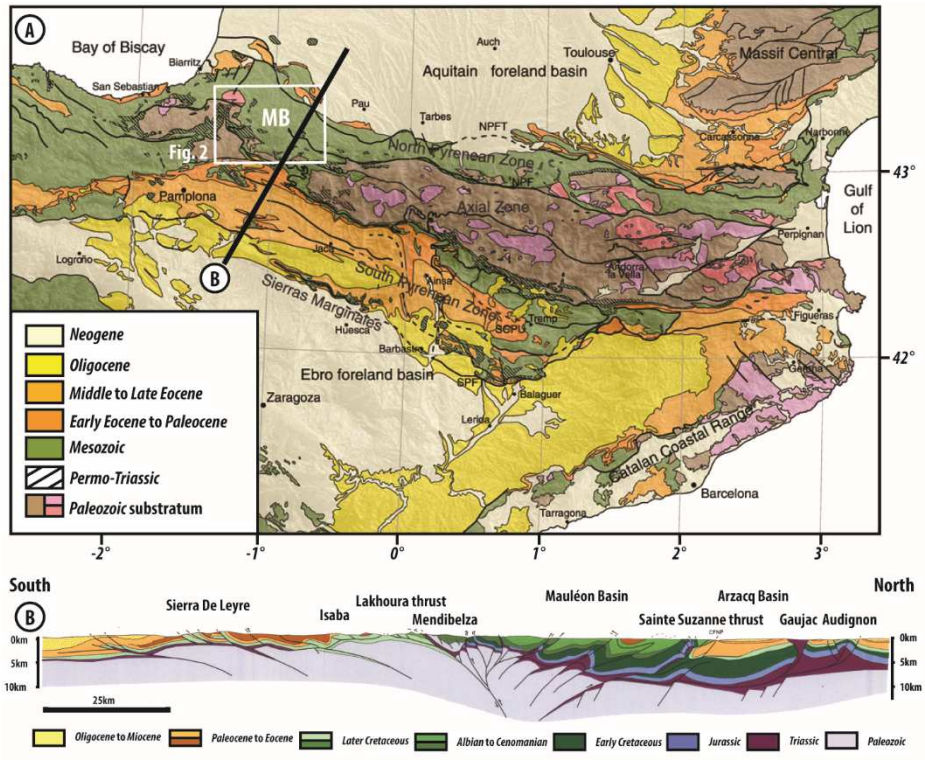

(A) Geological map of the Pyrenees showing the structural domains of the belt: North Pyrenean Zone, Axial Zone and South Pyrenean Zone (Mouthereau et al., 2014). NPFT: North Pyrenean Frontal Thrust; MB: Mauléon Basin; (B) Geological cross-section across the Western Pyrenees showing from north to south, the: *Audignon* Ridge, *Arzacq* Basin, *Mauléon* Basin, *Mendibelza* Unit, *Lakhoura* Thrust, *Isaba* Unit and *Sierra de Leyre* Unit (AGSO and BRGM., 2018).

Figure. 2

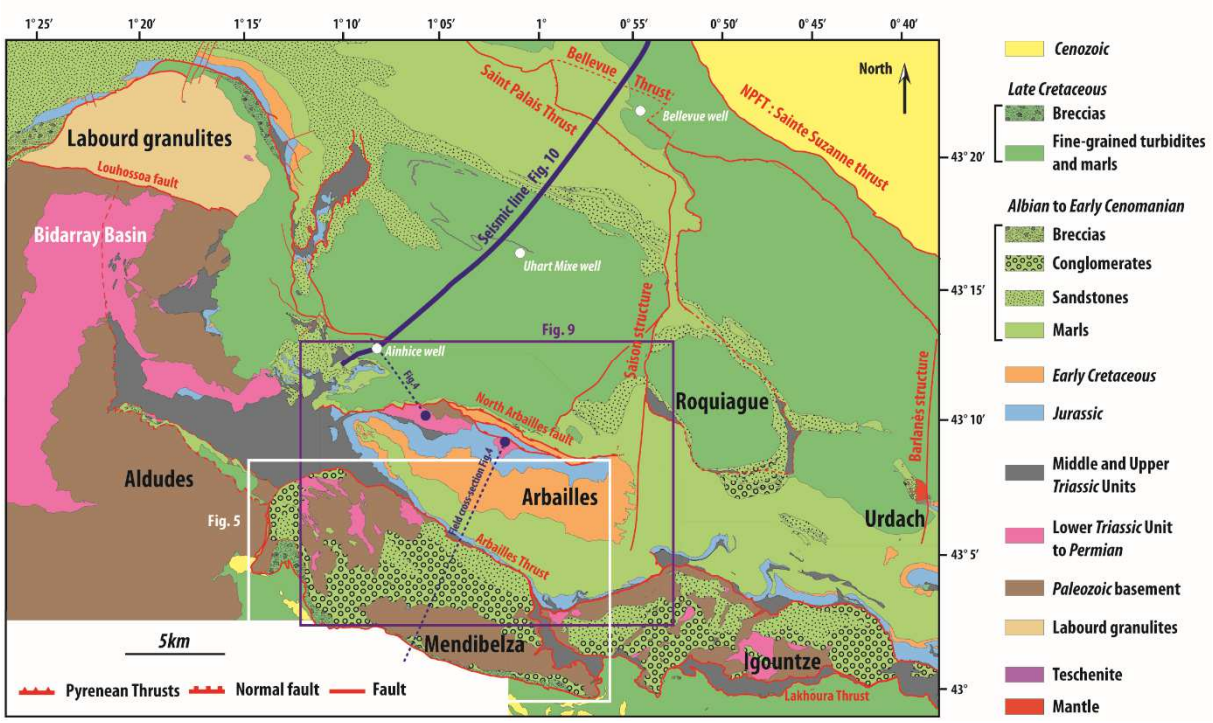

Geological map showing the main structural units of the Iberian *Mauléon* margin, from west to south: *Labourd* granulites, *Bidarray* Basin, *Aldudes* Unit, *Mendibelza-Igountze* Unit. The Mauléon Basin geological map presented in this paper derive from an update of the published 1/50 000 geological maps (Casteras et al., 1970, 1971; Boissonnas et al., 1974; Le Pochat et al., 1976, 1978; Henry et al., 1987).

Figure. 3

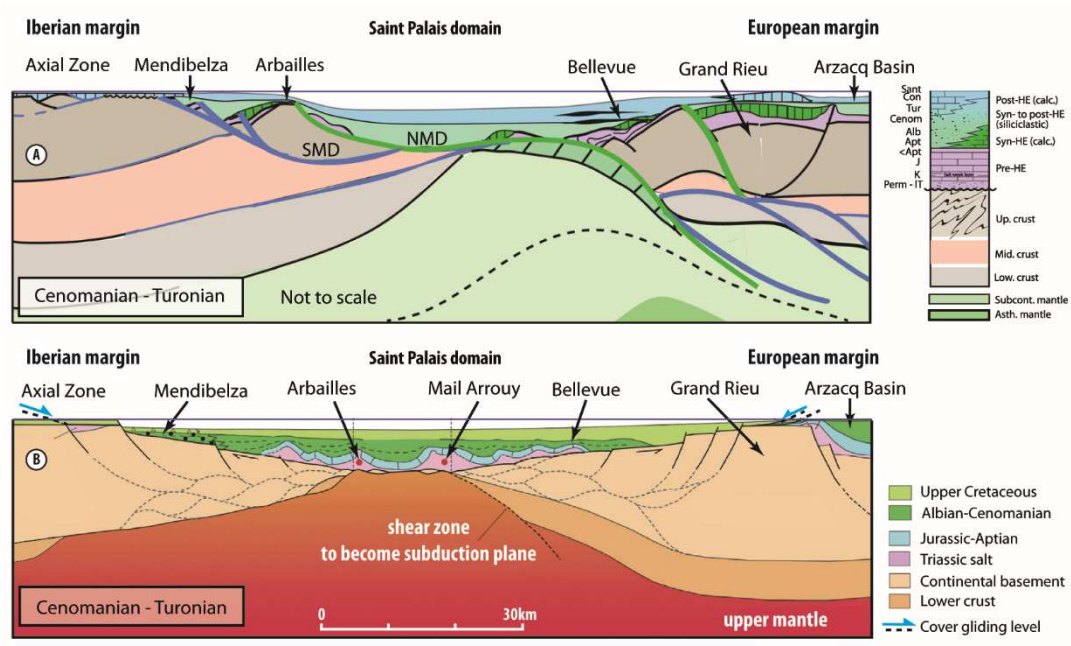

(A) 2D synthetic tectono-sedimentary model of the Mauléon-Arzacq rift section during the Cenomanian to Turonian post-tectonic stage (modified from Masini et al., 2014). The continental crust is thinned during Albian time as the result of the development of two diachronous northward dipping detachments. SMD: South Mauléon Detachment; NMD: North Mauléon Detachment; HE: Hyper-extension; (B) Late Cretaceous restoration of the Mauléon Basin. The dashed lines correspond to supposed anastomosed shear zones contributing to continental crust thinning (modified from Teixell et al., 2016). This model proposes a boudinage-like geometry of the crust, with narrow continental margins (<40 km wide).

1346 **Figure. 4**

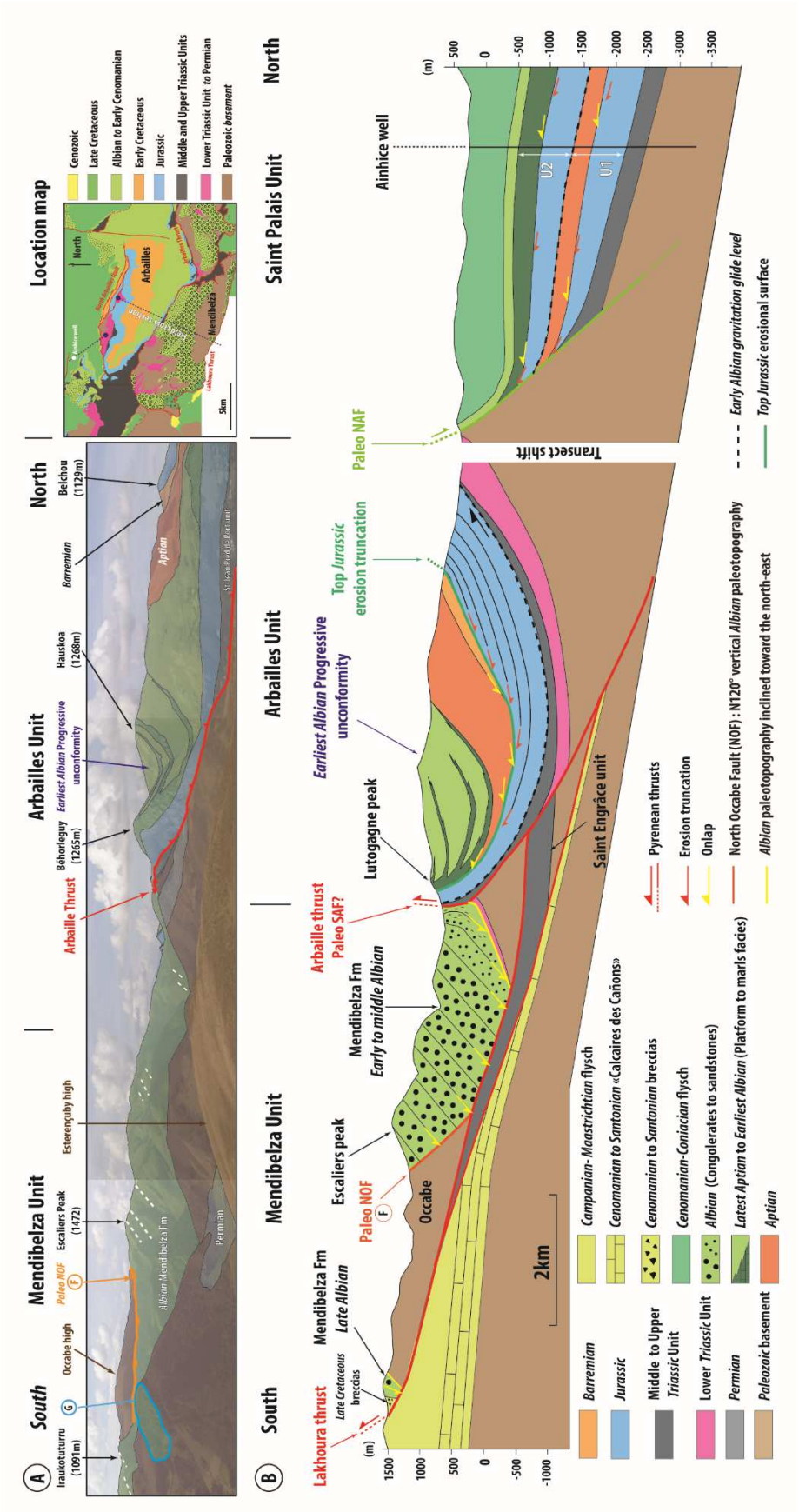

1347

(A) Panoramic view of the *Mendibelza* and *Arbailles* Units. The *Mendibelza* Formation is characterized by the absence of wedge-shaped syn-tectonic growth strata in the Albian synrift sequence and a N120°-30°SW orientation. These conglomerates stop on the Albian North *Occabe* paleo-normal fault (NOF) whose current orientation is N110°-45°N. The *Arbailles* Unit is characterized by a progressive unconformity affecting the Aptian to earliest Albian deposits, showing a northward inclination of the sedimentary profile at this time; (B) Current-day geological cross-section showing from north to south the: *Saint-Palais*, *Arbailles*, *Mendibelza*, *Saint-Engrâce*/Bedous and *Axial Zone* Units. The *Arbailles* Unit is characterized by Jurassic cover eroded to the south, overlain by a southward back-stepping Early Cretaceous carbonate platform. The *Arbailles* Unit is separated from the *Mendibelza* Unit by the steep *Arbailles* Thrust. The *Mendibelza* Unit overthrust the *Axial Zone* and the *Larrau*/*Saint-Engrâce* Units due to the *Lakhoura* Thrust.

Figure. 5

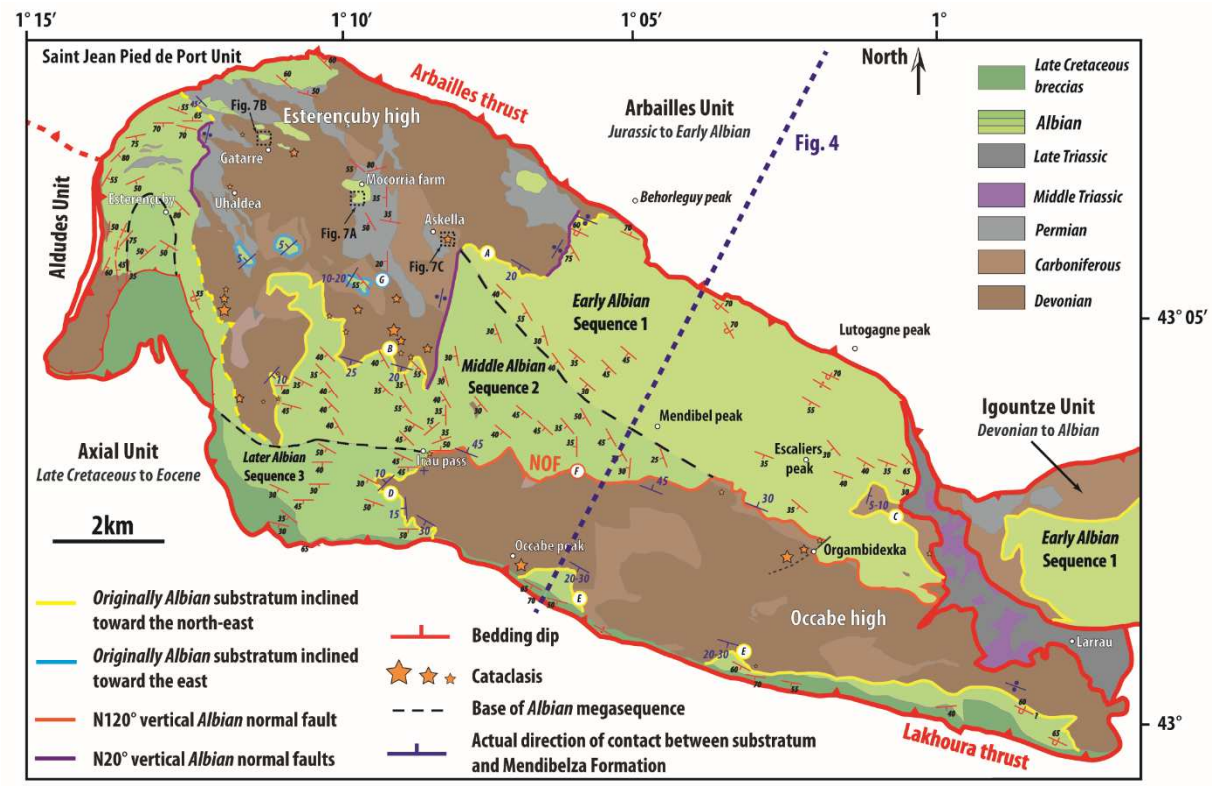

Geological map of the *Mendibelza* Unit, modified from the 1/50 000 BRGM geological maps (Casteras et al., 1970, 1971; Le Pochat et al., 1978). The *Mendibelza* Formation is composed of three main synrift mega-sequences, younger and younger towards the south, defined by Souquet et al. (1985). The stereographic representations show the Albian orientation of the contact between the *Mendibelza* conglomerates strata and the sedimentary basement. The *Mendibelza* Unit is separated from the *Arbailles* Unit by the steep *Arbailles* fault and is overthrust towards the south by the *Lakhoura* Thrust. The North Occabe Fault (NOF) is fossilized by the Albian Megasequences 1 and 2, indicating an Early to Middle Albian age for this fault.

1371 **Figure. 6**

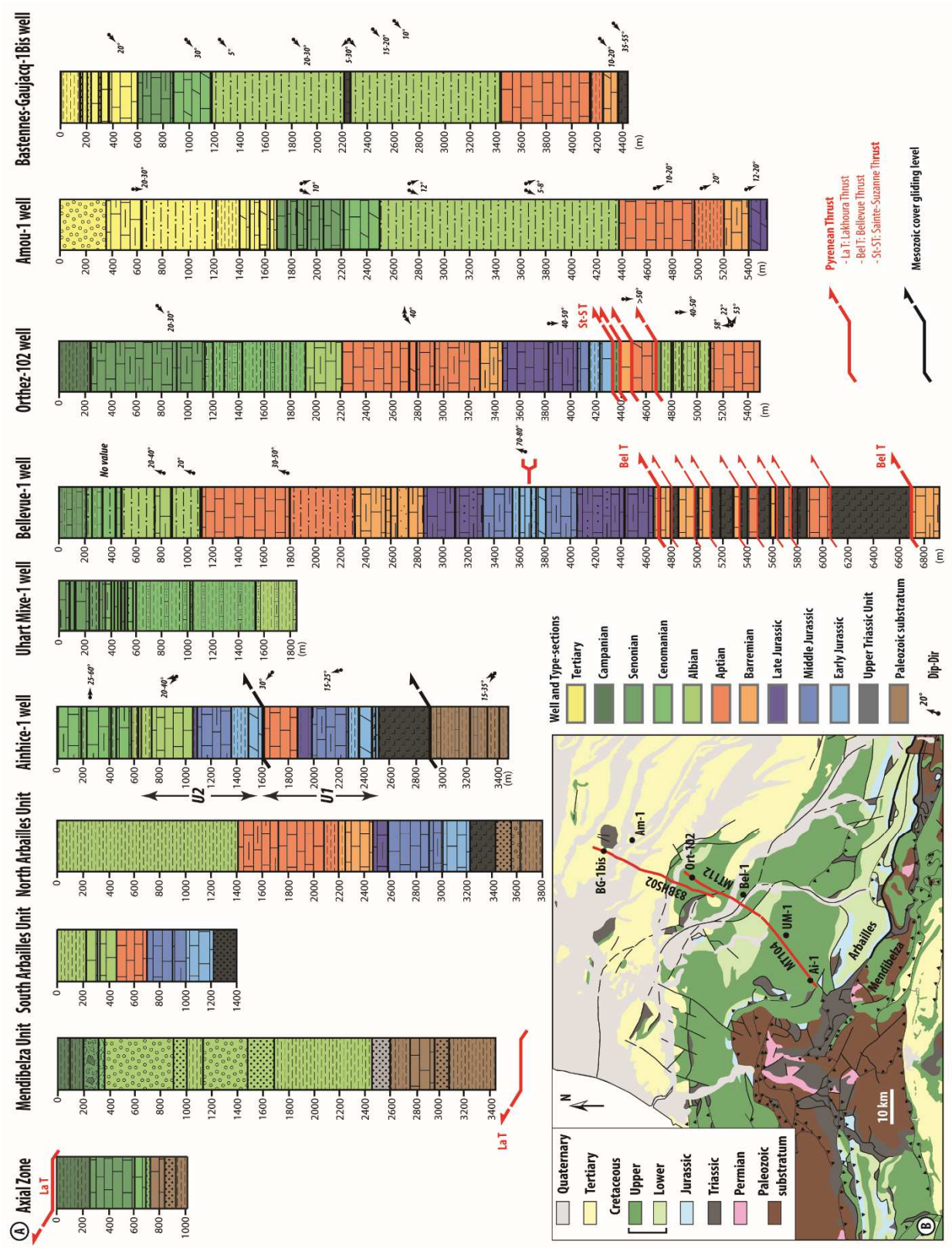

1372

(A) To the south: synthetic sedimentary succession of the Axial Zone, Mendibelza Unit, South Arbailles Unit and North Arbailles Unit; To the north: sedimentary facies of the six wells calibrating the interpreted N-S composite seismic reflection profile (Fig. 10). (B) Location of the N-S composite seismic reflection profile (Fig. 10) on the 1 / 400 000 BRGM geological map of Pyrenees (Baudin and Barnolas, 2008). From south to north the MT104, MT112 and 83HBS02 seismic lines. Ai-1: Ainhice-1 well, UM-1: Uhart Mixe-1 well, Bel-1: Bellevue-1 well, Ort-102: Orthez-102 well, Am-1: Amou-1 well and BG-1bis: Bastennes Gaujacq-1bis well.

1381 **Figure. 7**

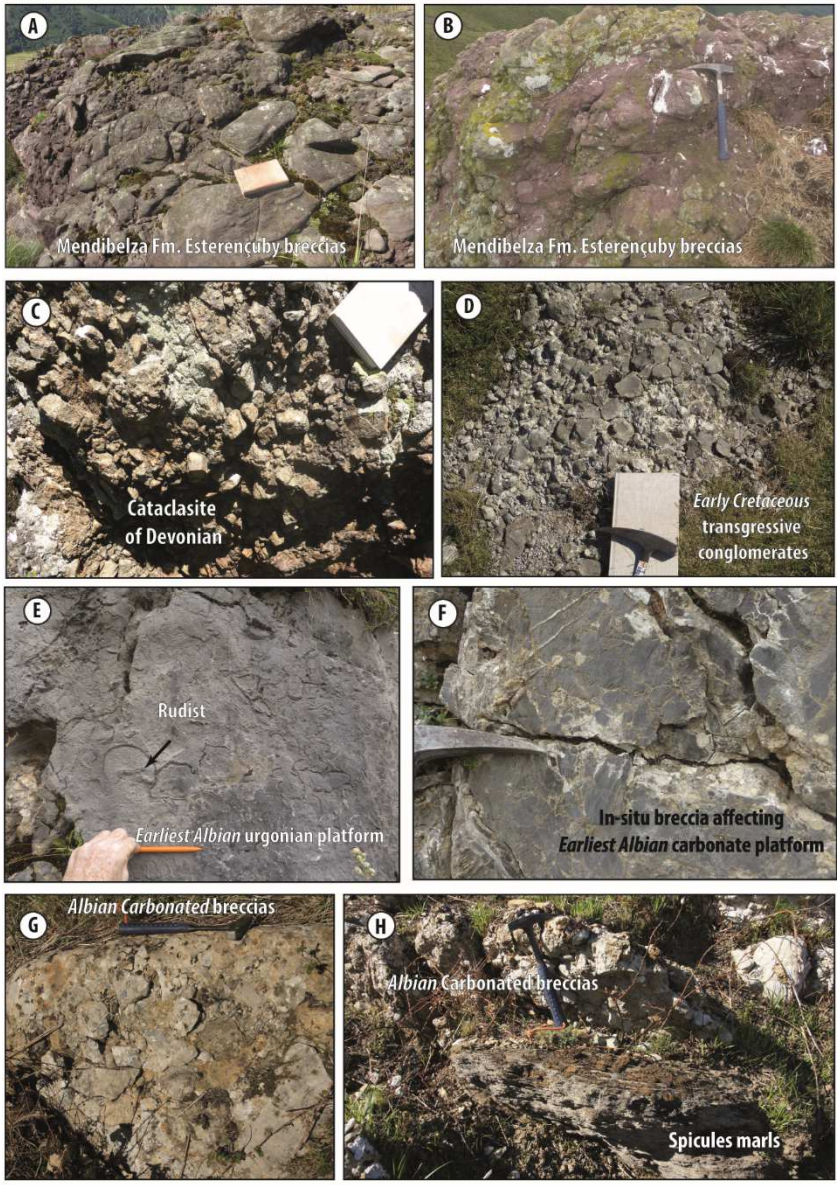

1382

1383 See Figs. 5 and 9 for location. (A-B) Early Albian *Esterençuby* breccias reworking the Lower
1384 Triassic Sandstone Unit. These discontinuous breccias are located at the base of the
1385 Megasequence one of the *Mendibelza* Formation defined by Souquet et al. (1985); (C)
1386 Cataclasites affecting the sedimentary Paleozoic basement of the Esterençuby high; (D) Early
1387 Cretaceous transgressive conglomerates reworking the Kimmeridgian carbonate deposits; (E)
1388 latest Aptian-earliest Albian "Mélobésiées" carbonate platform on the southern part of the
1389 *Arbailles* Syncline; (F) In-situ breccias of the Late Aptian-earliest Albian carbonate platform

deposits, due to the northward inclination of the sedimentary profile; (G-H) Carbonate breccias intercalated with spicule marls on the northern corner of the *Arbailles* Unit. These breccias correspond to the northward reworking of the Late Aptian-earliest Albian carbonate platform.

Figure. 8

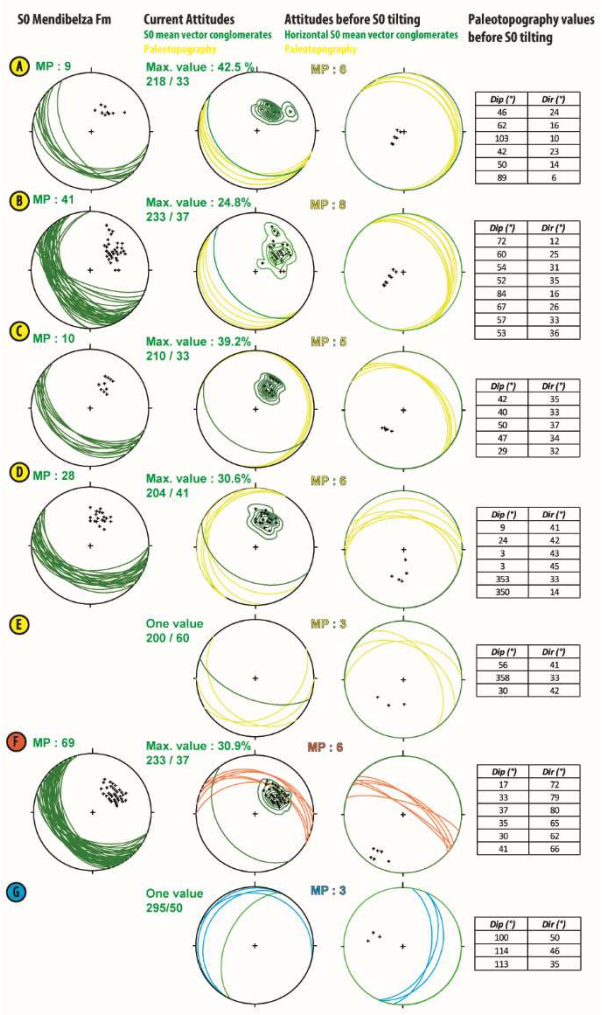

Stereographic representation of the structural data showing the current and the Albian orientation of the contacts between the *Mendibelza* conglomerates strata and the Paleozoic sedimentary basement of the *Mendibelza* Unit. The sites are localized on the map Fig 5. The first column represents the current *Mendibelza* Formation strata. Second column shows the current orientation of the contacts between Mendibelza Formation strata and the Paleozoic basement. The third column shows the Albian orientation of the contacts. The average value of the Albian yellow surface is N131-35°NE. The NOF represented by the site F is characterized by a sub-vertical Albian orientation. MP: Measurements planes.

1404 **Figure. 9**

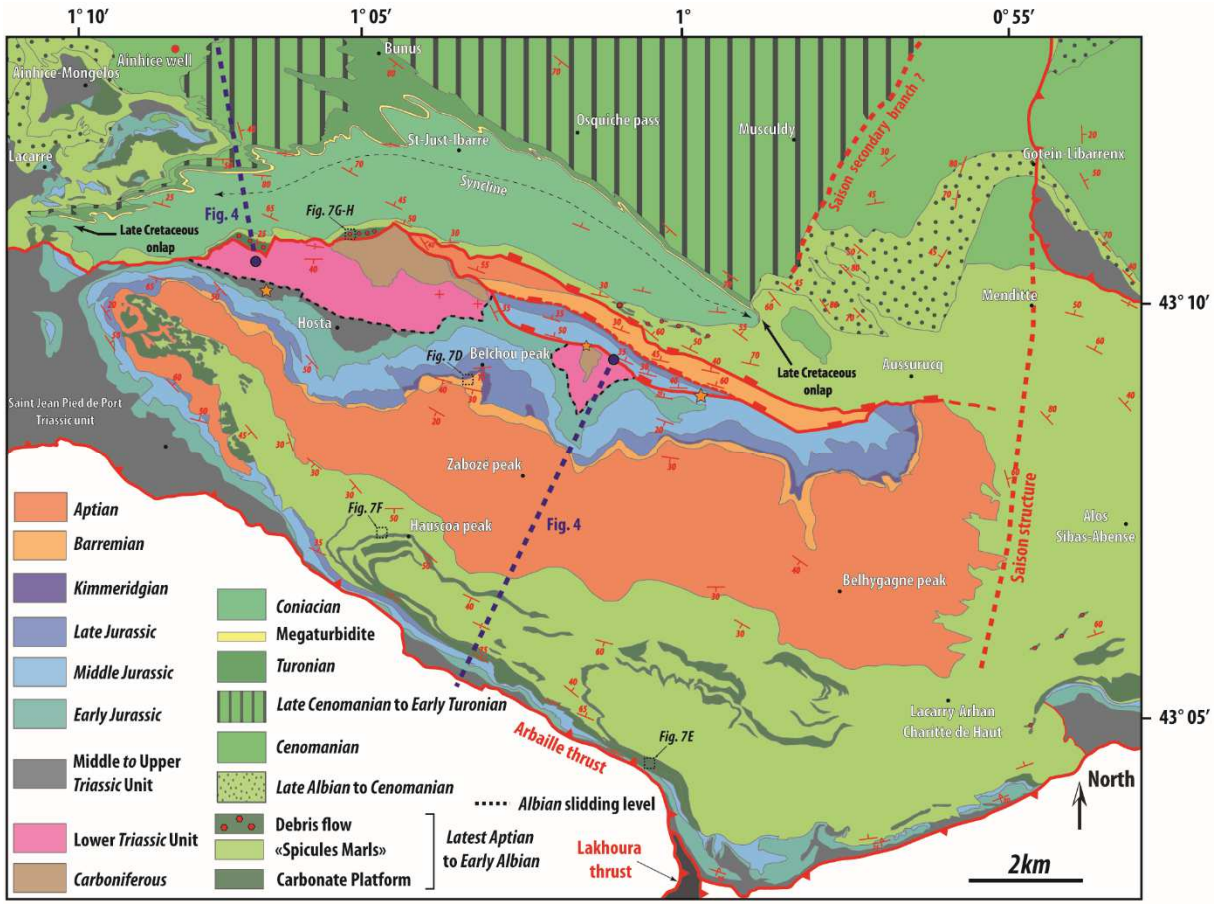

1405

1406 Geological map of the *Arbailles* Unit and the southern part of the *Saint-Palais* Unit, using
1407 updated BRGM 1/50 000 maps (Casteras et al., 1971; Boissonnas et al., 1974; Le Pochat et
1408 al., 1976, 1978). The *Arbailles* Unit is separated from the *Saint-Palais* Unit by N120° normal
1409 faults known as the North Arbailles Fault (NAF). These maps highlight the southward erosion
1410 of the Jurassic cover and the southward back stepping of the Barremian to Aptian carbonate
1411 platform, onlapping the previous eroded Jurassic deposits. In the North of the *Arbailles* Unit,
1412 the Late Cretaceous deposits onlapped the Albian rift sequence towards the south from
1413 Cenomanian to Santonian time.

1414 **Figure. 10**

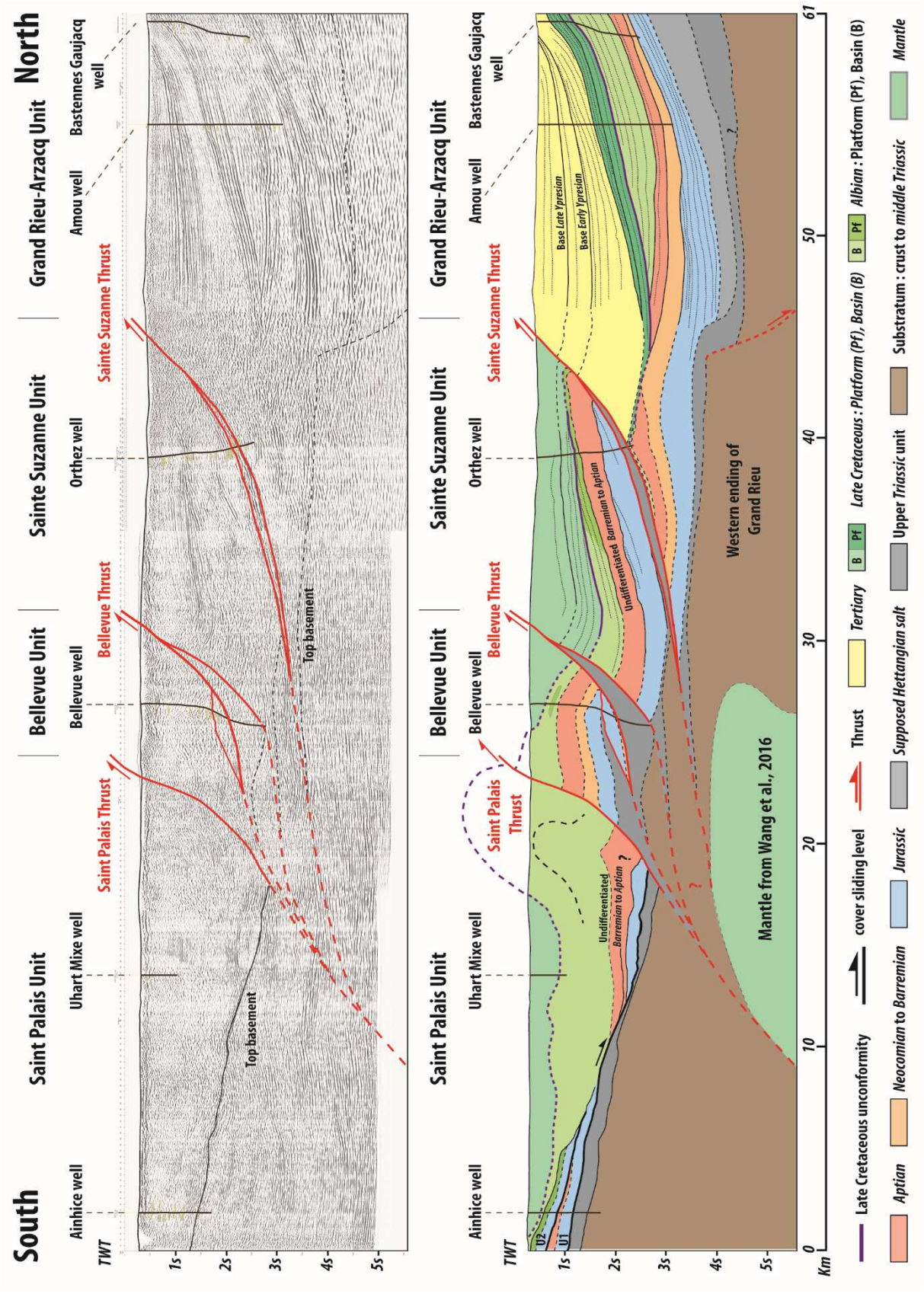

1415

Interpretation of a N-S petroleum reflection composite seismic line, reprocessed by the BRGM in 2017 (MT104, MT112 and 83HBS02). This composite seismic line shows the deep geometry of the *Mauléon* Basin and its European margin. This seismic line through the *Mauléon* Basin cuts across four distinct structural units, separated from one another by thrusting overlaps. From south to north, the units are as follows: (1) *Saint-Palais,* (2) *Bellevue,* (3) *Sainte Suzanne,* and (4) *Grand-Rieu/Arzacq*. The *Saint-Palais* Unit corresponds to the Albian rift depocenter. The *Bellevue* and *Sainte Suzanne* Units materialized the northern conjugate margin of the Albian Cretaceous *Mauléon* rift basin, and the Barremian-Aptian depocenter.

Figure. 11

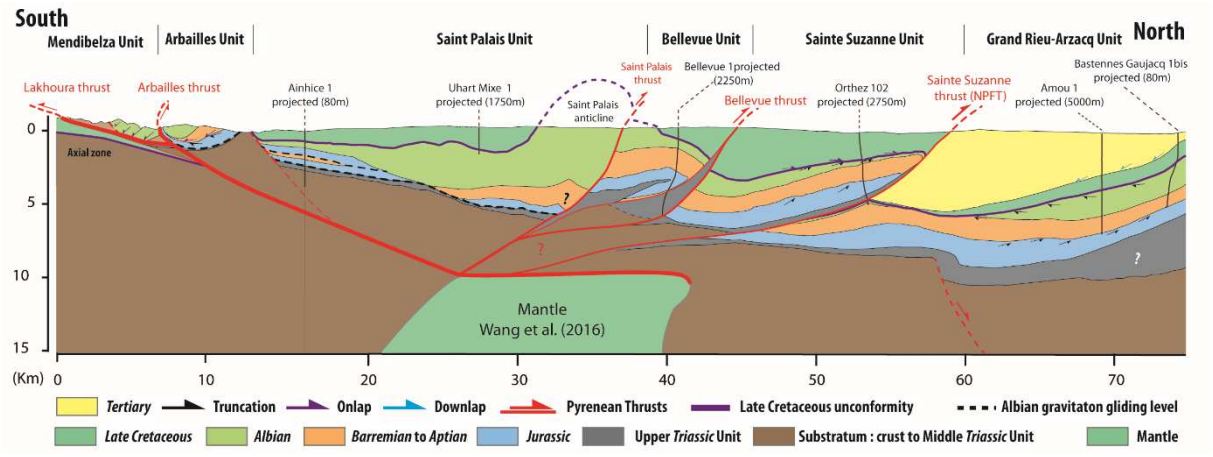

N-S Composite cross-section of the *Mauléon* Basin. The southern part corresponds to the field cross-section Fig. 4 and the northern part of the section is calibrated by the seismic line. The *Mendibelza* and *Arbailles* Units correspond to the southern margin of the *Mauléon* Basin. The *Saint-Palais* Unit represents the Albian rift depocenter. The *Bellevue* and *Sainte Suzanne* Units materialized the northern rift margin of the *Mauléon* Basin and are northward overthrust onto the *Arzacq* Basin.

Figure. 12

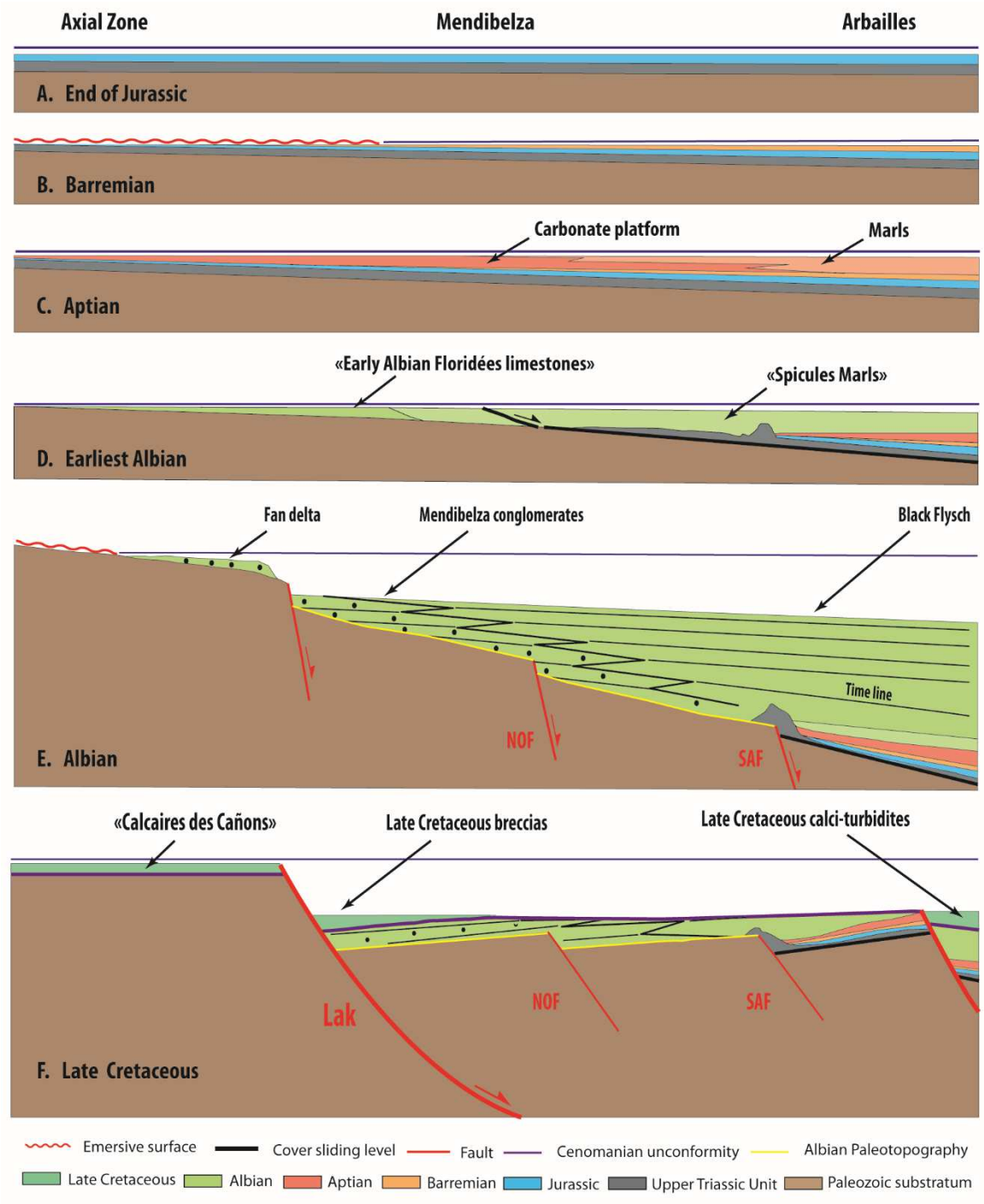

Schematic tectono-sedimentary evolution of the southern margin of the *Mauléon* Basin from the end of Jurassic to Late Cretaceous time. (A) During the Jurassic, this domain is characterized by the development of a carbonate platform. (B) The Jurassic platform underwent an emersion phase from the end of Jurassic to the base of Barremian time. This

1439 emersive phase was responsible for erosion of the previous carbonate platform, as shown by
1440 the southward erosional truncations affecting the Jurassic under the Early Cretaceous
1441 deposits. (C) The Early Cretaceous is characterized by a lack of Neocomian and the
1442 development of a flat carbonate platform during Barremian-Early Aptian time. During Late
1443 Aptian time, the previous carbonate platform distalized towards the north into more distal
1444 spicule marls, showing a slight tilt of the depositional profile. (D) At Early Albian time, the
1445 southern *Mauléon* margin was affected by the gravitational sliding of the Mesozoic cover
1446 towards the north leading to local diapirism. (E) The Albian time was characterized by
1447 differential vertical movements responsible for the uplift of the southern margin and tectonic
1448 subsidence towards the north. This stage is materialized by the sedimentation of the
1449 *Mendibelza* Fm. proximal turbiditic s.l. siliciclastic system, onlapping towards the south a
1450 Paleozoic basement inclined towards the north. The northward tilt of the Iberian margin is
1451 affected by southward propagating N120° normal faults. (F) At Cenomanian time, the
1452 *Mendibelza-Arbailles* Unit was affected by a tilt towards the south.

Figure. 13

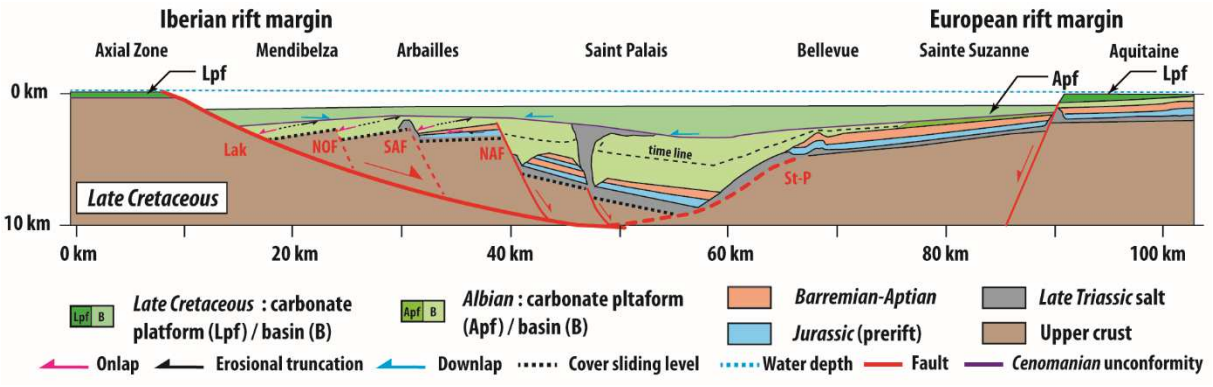

Schematic cross-section of the *Mauléon* Basin during Late Cretaceous showing the asymmetry of the rift basin margins and the geometry of the Cretaceous deposits. Lak: Lakhoura detachment, NOF: North *Occabe* fault, SAF: South Arbailles fault, NAF: North *Arbailles* fault, St-P: *Saint-Palais* detachement.

Figure. 14

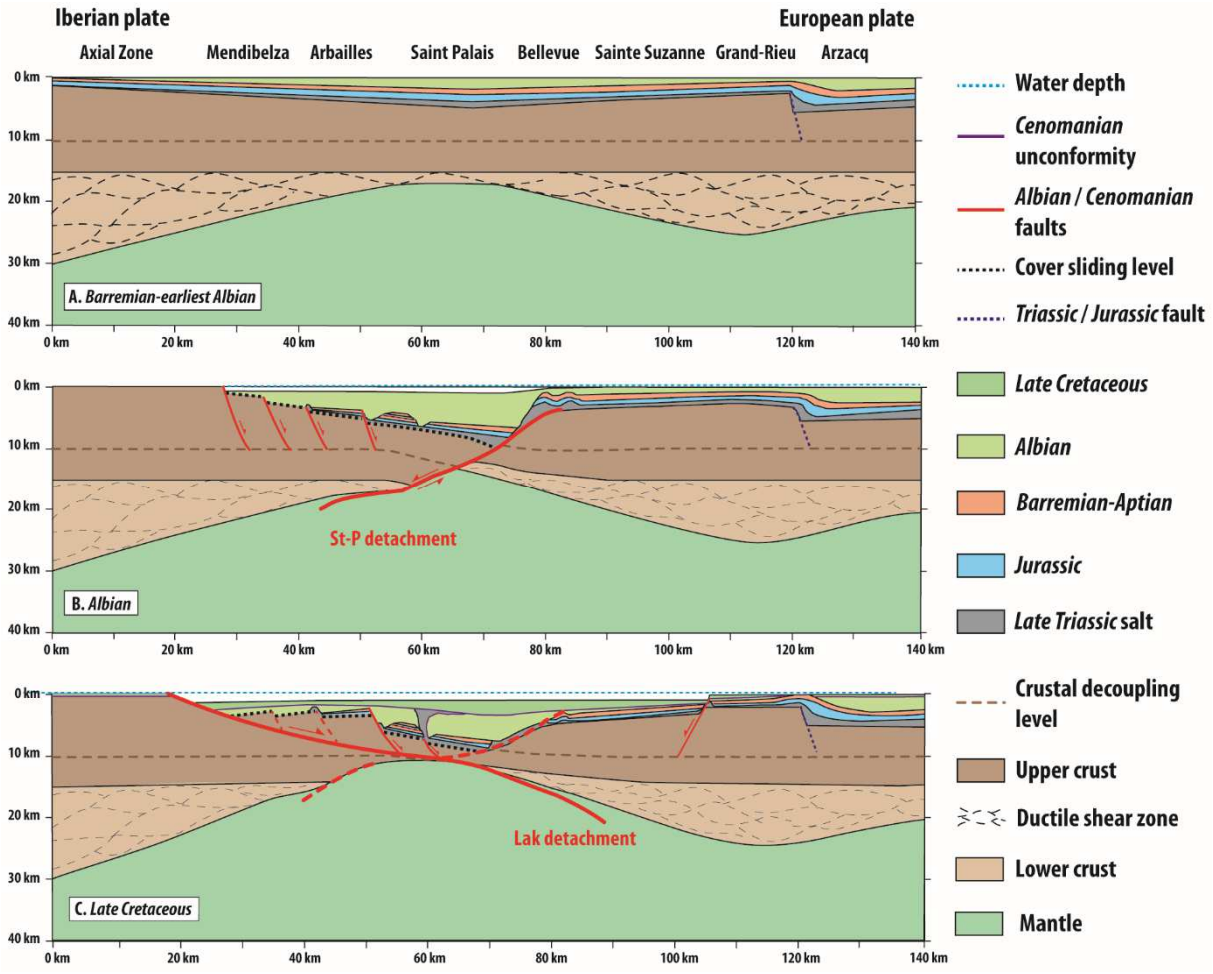

Geodynamical model of crustal thinning of the *Mauléon* hyper-thinned rift basin. The genesis of the *Mauléon* Basin comprises two lithospheric thinning stages. (A) Barremian to Aptian rifting stage 1: "ductile pure-shear thinning phase" affecting mainly the lower crust, inducing the formation of a symmetric synrift sag basin. (B) Albian rifting stage 2: simple-shear thinning phase inducing the development of an asymmetric synrift basin, characterized by proximal turbiditic system on the southern margin and carbonate platform deposits on the northern one. The *Saint-Palais* southward detachment fault is responsible for the hyper-thinning of the sub-continental crust during Albian time. (C) Early Cenomanian rifting stage 3: the southern margin was tilted towards the south along a northward dipping detachment

fault responsible for local sub-continental mantle denudation, resulting in the formation of an apparent symmetric rift basin. St-P: *Saint-Palais*, Lak: *Lakhoura*.